ACR No. 4H31

NATIONAL ADVISORY COMMITTEE FOR AERONAUTICS

WARTIME REPORT

ORIGINALLY ISSUED

August 1944 as
Advance Confidential Report 4H31

AN ANALYTICAL INVESTIGATION OF THERMAL-ELECTRIC MEANS OF PREVENTING ICE FORMATIONS ON A PROPELLER BLADE

By Richard Scherrer

Ames Aeronautical Laboratory
Moffett Field, Calif.

NACA

WASHINGTON

NACA ACR No. 4H31

NATIONAL ADVISORY COMMITTEE FOR AERONAUTICS

ADVANCE CONFIDENTIAL REPORT

AN ANALYTICAL INVESTIGATION OF THERMAL-ELECTRIC MEANS OF PREVENTING ICE FORMATIONS ON A PROPELLER BLADE

By Richard Scherrer

SUMMARY

Thermal-electric means of preventing ice formations on a propeller blade have been investigated and a theoretical basis for the continued development of thermal-electric blade shoes is provided.

A method is presented that can be applied to the design of thermal-electric blade shoes for any propeller or rotor, and an optimum heat distribution is determined for a propeller blade.

INTRODUCTION

The design and development of suitable thermal ice-prevention equipment for aircraft propellers have been undertaken as a part of a general research program concerning ice-prevention equipment for aircraft.

The National Research Council of Canada has conducted flight tests, under natural icing conditions, of propellers equipped with electrically heated blade shoes (reference 1). These results formed the basis of the preliminary blade-shoe designs used during flight tests conducted by the NACA in the vicinity of Minneapolis, Minn., during the winter of 1942-43 (reference 2). The blade shoes tested by the National Research Council of Canada and the NACA consisted of a layer of neoprene serving as thermal and electric insulator bonded to the propeller blade with an outer layer of electrically

conductive neoprene bonded to the insulating layer. (See fig. 1.) The power was supplied to these blade shoes through radial wires between the neoprene layers at the rear edges of the shoe. Flight tests with electrically heated propeller-blade shoes reported in references 1 and 2 have established the practicability of protecting propeller blades from ice formations by thermal-electric means. The data of references 1 and 2 indicate that the power required for ice prevention may be excessive for certain applications, although sufficient power for some degree of ice removal may be provided readily. The analysis reported herein provides a rational basis for establishing thermal-electric propeller-blade-shoe designs.

SYMBOLS

The following symbols have been used in this analysis:

A	aspect ratio
B	number of propeller blades
D	propeller diameter, feet
J	work equivalent, 778 foot-pounds per Btu
Nu_δ	boundary-layer Nusselt number based on the laminar boundary-layer thickness, $h\delta/k$
P	normal pressure coefficient on airfoil section
P_a	normal pressure coefficient due to the additional lift distribution
P_b	normal pressure coefficient due to the basic lift distribution
P_r	reference profile pressure coefficient
Q	heat quantity, Btu per hour or watts
R	propeller radius, feet
R_c	Reynolds number based on blade chord, $V_R c/\nu$

R_d Reynolds number based on leading-edge diameter, $V_R d/\nu$

R_i rate-of-icing ratio

S area, square feet (unless otherwise noted)

T temperature, degrees Fahrenheit

T_A temperature rise due to aerodynamic heating, degrees Fahrenheit

V velocity just outside of the boundary layer, feet per second

V_M maximum local velocity, feet per second

V_f local velocity due to airfoil shape, feet per second

V_o forward velocity of propeller, feet per second

V_R resultant velocity of the blade section, feet per second

V_r local velocity on the reference profile, feet per second

V_s local velocity at the laminar separation point, feet per second

W water content of the air stream, pounds of water per cubic foot of air

a slope of the lift curve for any blade section

a_o slope of the lift curve at infinite aspect ratio

b chordwise distance through which heat is conducted, feet

c blade chord, feet

c_l propeller-blade section lift coefficient

c_{l_a} additional section lift coefficient

c_{l_b} basic section lift coefficient

c_{p_a} specific heat of air, Btu per pound, degrees Fahrenheit

c_p specific heat of water, Btu per pound, degrees Fahrenheit

d leading-edge diameter, feet

g acceleration due to gravity, 32.2 feet per second per second

h heat-transfer coefficient, Btu per hour, square foot, degrees Fahrenheit

k thermal conductivity, Btu per hour, square foot, degrees Fahrenheit per foot

l distance from the edge of an ice layer, feet

m distance normal to blade-shoe surface, feet

n propeller speed, revolutions per second

p absolute value of the ratio of the slopes of a double-roof velocity profile

q heat per unit area, Btu per hour, square foot or watts per square inch (as noted)

r blade station radius, feet

s chordwise distance along the airfoil surface from the stagnation point, feet

t thickness, feet

x distance along the airfoil chord line, feet

Φ helix angle, degrees

Φ_M helix angle at 0.75R at $(V_o/nD)_{max}$, degrees

Ω angular velocity of the blade, radians per second

α angle of attack, degrees

α_{l_o} angle of zero lift, degrees

β blade angle measured from the plane of rotation, degrees

δ laminar boundary-layer thickness from the surface to the point at which $V = 0.707\ V_R$, feet

δ_T heat-transfer characteristic length for a turbulent boundary layer

ζ turbulent boundary-layer parameter

θ blade angle at any radius, degrees

θ_M blade angle at 0.75R at $(V_o/nD)_{max}$, degrees

ν kinematic viscosity, square feet per second

ψ ice-thickness parameter

Subscripts

I insulation

L lower surface of the blade

U upper surface of the blade

b blade

h blade root

i ice

s laminar-separation point

t blade tip

u leading edge of the blade shoe

v rear edge of the blade-shoe conducting layer

w trailing edge of the blade

as blade surface aft of the blade shoe

bs blade shoe

cl conducting layer

cs blade-element radial cross section

stag stagnation-pressure region

o ambient air

1 a point on the blade or shoe surface

a a point in the blade shoe

0.75 r/R = 0.75

+ positive values of λ

- negative values of λ

METHOD

An optimum design of a propeller-blade shoe should provide equal protection to all points on the blade-shoe surface at the design conditions and have the minimum permissible total power input. The method of analysis presented hereinafter is general in scope and can readily be applied in the design of an optimum blade-shoe arrangement for any propeller or rotor blade.

In this analysis the blade shoe is considered to extend radially from the propeller-blade root, station $(r/R)_h$, to the propeller-blade tip, station $(r/R)_t$, and chordwise from the blade leading edge, station $(s/c)_u$, to station $(s/c)_v$ on both the upper and lower surfaces of the forward portion of the blade. (See fig. 1.) Heat is considered to be applied to this portion of the blade while the after portion, extending from station $(s/c)_v$ to the propeller trailing edge, station $(s/c)_w$, is neither heated nor covered. The blade shoe is considered to be comprised of an inner layer, adjacent to the propeller-blade surface, of an insulating rubberlike material of thickness t_I overlaid with an electrically conductive layer of similar material of thickness $t_{c\ell}$. The use of an additional thin layer of insulating material over the conducting layer to increase the resistance to abrasion will not be considered in the analysis; however, the effect of such a layer can be determined readily.

Ice protection may be accomplished by two different processes: (1) ice can be prevented from forming, and (2)

ice can be removed periodically in thin layers. To provide for ice prevention on propeller blades, it is necessary to supply sufficient heat to maintain the temperature of the blade-shoe surface above 32° F in any atmospheric condition. Protection by ice removal can be effected by providing sufficient heat to raise the blade-shoe surface temperature above 32° F only after ice has formed. It can be seen that the removal process involves thermal economies by utilizing the insulating properties of ice to reduce the convection losses and to obviate the need of supplying the heat of fusion and the heat of evaporation.

The total power required for either ice prevention or ice removal is dependent upon the atmospheric conditions, the propeller-operating conditions, and the propeller design, and may be expressed as the summation of the heat required to prevent or remove ice formations on the propeller-blade-shoe surface and the heat lost through the after or uncovered portion of the propeller blade. The heat required to prevent or remove ice on the blade-shoe surface Q_{bs} is the summation, over the radial and chordwise extent of the blade-shoe surface, of the values of unit heat (heat per unit area) required for the prevention or removal of ice at each point on the blade-shoe surface q_{bs}. Likewise the heat lost through the after surface of the propeller blade Q_{as} is the summation, over the radial and chordwise extent of the uncovered portion of the propeller blade, of the values of unit heat lost at each point on the after portion of the blade q_{as}.

The unit heat required to prevent or remove ice at each point on the blade-shoe surface q_{bs} is dependent upon (1) the surface heat-transfer coefficient, (2) the water content of the air stream, (3) the ambient-air temperature, and (4) the resultant velocity and effective angle of attack of the propeller-blade section. The unit heat loss q_{as} at each point on the after surface of the propeller blade is a function of (1) the surface heat-transfer coefficient, (2) the ambient-air temperature, (3) the thermal conductivities of the propeller-blade and blade-shoe materials, and (4) the resultant velocity and effective angle of attack of the propeller-blade section.

The method of analysis which follows is therefore concerned with the determination of these various factors which are necessary to evaluate q_{bs} and q_{as} and thereby effect

a solution for the total power required and for the optimum heat distribution for the specific application.

Determination of the Surface Heat-Transfer Coefficients

The subject of heat transfer from airfoils has been widely investigated and several approaches to the subject have been developed. Since each section of a propeller blade is essentially an airfoil section, the method of determining the surface heat-transfer coefficients of an airfoil section has been utilized in the solution of the surface heat-transfer coefficients of a propeller blade.

The surface heat-transfer coefficients of an airfoil section are dependent upon the physical characteristics of the airfoil boundary layer, and therefore its determination requires a knowledge of the location along the airfoil surface of the point of transition of the boundary layer from laminar to turbulent flow as well as of the boundary-layer thickness along the airfoil surface.

Propeller-blade section velocity distribution.- Since the extent of the laminar boundary layer for a specific airfoil section - or, as in this analysis, a specific propeller-blade section - is dependent upon section velocity distribution, one of the first steps in the determination of the propeller-blade surface heat-transfer coefficients is the determination of the velocity distribution for the propeller-blade sections under consideration. The velocity distribution for any propeller-blade section is determined by the lift coefficient and angle of attack at which that blade section is operating. The angle of attack of each propeller-blade section can be written as the difference between the blade angle and the helix angle at the blade station considered,

$$\alpha = \beta - \Phi \tag{1}$$

and the lift coefficients for each propeller-blade section can be determined by correcting the section lift-coefficient curves for the effect of finite aspect ratio. The effective aspect ratio for each blade section can be obtained from the following equation:

$$A = \frac{8}{\pi\sigma_0}\frac{r}{R}\frac{V_R}{\sqrt{V_R^2 + r^2\Omega^2}} \tag{2}$$

which is developed in reference 3, and in which

$$\sigma_0 = \frac{Bc}{\pi R}$$

From the effective aspect ratio, the correct lift-curve slopes can be computed by the equation

$$a = \frac{a_0}{1 + \frac{a_0 \times 57.3}{\pi A}} \tag{3}$$

and the correct lift coefficients obtained by the relation

$$c_l = a(\alpha - \alpha_{l_0}) \tag{4}$$

If the lift coefficient and angle of attack are known, the velocity distribution over each propeller-blade section can be determined by the method of either reference 4 or 5.

Laminar boundary layer.- The extent of the laminar boundary layer is a function of the blade-section velocity distribution and the boundary-layer Reynolds number. For the purpose of this report, the boundary layer will be considered laminar from stagnation to the laminar-separation point and then turbulent to the trailing edge. The method of locating the laminar-separation point is developed from the theory by Von Kármán and Millikan (reference 6). By expressing the relation of reference 6 in the nomenclature of this report, the following equation is obtained:

$$\frac{V_s}{V_M} = \left[1 - p(X - 1)\right]^{\frac{1}{6}} \tag{5}$$

in which X is equal to θ_s of reference 6 and is explicitly defined therein. The absolute value of the ratio of the slopes of the double-roof velocity profiles, which are drawn to approximate the actual velocity profiles, is p and the curve for V_s/V_M as a function of p is plotted in figure 2.

The heat transfer in a laminar boundary layer is shown in reference 7 as being dependent on the boundary-layer Nusselt number and is a function of the boundary-layer thickness δ and the thermal conductivity of air k. In the relation

$$\frac{h\delta}{k} = Nu_\delta \tag{6}$$

Nu_δ is a function of the shape of the boundary-layer velocity profile and Prandtl number and has a value of 0.765 for the Blasius-type boundary-layer velocity profile for air. Experiment has shown that, over the forward portion of an airfoil where a favorable pressure gradient exists, the Blasius-type boundary-layer velocity profile is closely approximated. At points on the surface of a body downstream of the minimum-pressure point, a laminar boundary layer exhibits a tendency to separate. Since the velocity gradient at the surface decreases as separation develops, the value of Nu_δ must diminish until at the separation point its value is zero. It is considered that reducing Nu_δ linearly from the minimum-pressure point to the separation point will satisfactorily approximate the actual case. Accordingly, in the analysis of this report Nu_δ has been considered to have a constant value of 0.765 from the stagnation-pressure region to the minimum-pressure point (maximum velocity) and then to vary linearly to zero at the laminar separation point.

The laminar boundary-layer thickness at any point s_1, as used in reference 7, is given by the equation

$$\delta^2 = \frac{5.3c^2}{R_c}\left(\frac{s_1/c}{V_1/V_R}\right)\left[\frac{\int_0^{s_1/c}\left(\frac{V}{V_R}\right)^{8.17} d\left(\frac{s}{c}\right)}{\left(\frac{V_1}{V_R}\right)^{8.17}\frac{s_1}{c}}\right] \tag{7}$$

which can be changed to the form

$$\delta = \left[\frac{5.3c^2}{R_c}\right]^{\frac{1}{8}}\left[\left(\frac{V_R}{V_1}\right)^{8.17} \times \int_0^{s_1/c}\left(\frac{V}{V_R}\right)^{8.17} d\left(\frac{s}{c}\right)\right]^{\frac{1}{8}} \tag{8}$$

to simplify the computations. Equation (8) is theoretically applicable only to Blasius-type boundary-layer profiles (stagnation to minimum-pressure point), but, as noted in reference 7, experiment has shown that little error is caused by its use to the laminar-separation point.

With the above method the solution for the boundary-layer thickness at the stagnation region becomes indeterminate; therefore, another method must be used to determine the heat-transfer coefficient in this region. The expression

$$\delta_{stag} = c\sqrt{\frac{1}{5R_c}\left(\frac{\bar{r}}{c}\right)} \tag{9}$$

also from reference 7, gives a satisfactory value for the boundary-layer thickness in this region based on the local radius of curvature $\bar{r}$, which is not necessarily the leading-edge radius.

Turbulent boundary layer.- The values of the heat-transfer coefficients for the turbulent boundary layer may be obtained by the method of reference 8. The surface heat-transfer coefficient h is defined in reference 8 by the equation

$$h = 0.76\,\frac{k}{\delta_T} \tag{10}$$

and the value of δ_T, the function of the turbulent boundary-layer thickness, is given by the equation

$$\delta_T = \frac{\zeta^2 c}{R_c\left(\frac{V}{V_R}\right)} \tag{11}$$

in which ζ is a turbulent boundary-layer parameter. The value of ζ at any point on the airfoil surface downstream from the laminar-separation point is obtained by a step-by-step solution of the equation

$$\frac{d\zeta}{dx} + \frac{6.13}{V}\frac{dV}{dx} = \frac{V}{\nu} f[\zeta] \tag{12}$$

from the point of laminar separation. The value of ζ at laminar separation is obtained from

$$\zeta = 2.557 \log_e \left[4.057 \, V_s \frac{0.289 \, \delta}{\nu} \right] \qquad (13)$$

Equation (12) has been rewritten in the form

$$d\zeta = d\left(\frac{x}{c}\right) \left[- \frac{6.13}{(V/V_R)} \frac{d(V/V_R)}{d(x/c)} + \frac{V_R c}{\nu} \left(\frac{V}{V_R}\right) f(\zeta) \right] \qquad (14)$$

for ease of computation. The values of $f(\zeta)$ as related to ζ are plotted in figure 3. A simplified method of applying the turbulent boundary-layer equations to obtain the value of δ_T at any point directly is presented in reference 9.

Heat Required for Ice Prevention

When the surface of a blade shoe covering the leading-edge portion of a propeller blade is heated to 32° F by applying power to the electric conducting layer, there will be some heat loss through the insulating layer and blade material to the air stream over the uncovered aft portion of the blade. The total power required to protect the propeller blade will then be that required to maintain a 32° F blade-shoe surface temperature plus the heat lost through the aft portion of the blade surface.

Heat required to maintain the blade-shoe surface at 32° F.- The heat necessary to maintain the blade surface at 32° F in icing conditions is a function of the surface heat-transfer coefficient h, ambient-air temperature T_o, temperature rise due to aerodynamic heating T_A, weight of water in each unit volume of air W, and the resultant velocity of each element of the propeller blade V_R.

The unit heat required is given by the relation

$$q_{bs} = h(32-T_o-T_A) + W V_R c_p (32-T_o)(3600) - \frac{W V_R^3}{2Jg} (3600) \qquad (15)$$

in which the first term is the heat transferred to the air flowing over the blade, if the blade is maintained at 32° F,

and the values of h are those that were determined in the previous section. The temperature difference between the blade surface and the ambient-air stream will be decreased by the amount of the temperature rise T_A caused by air flowing over the blade or being stopped in the stagnation region. The second term of equation (15) is the heat required to raise the temperature of all the water that strikes the blade to 32° F. The third term is the heat equivalent of the kinetic energy of the water striking the blade. The value of 3600, by which the second and third factors in equation (15) are multiplied, is to obtain dimensional consistency so that the units of q_{bs} are Btu per hour, square foot.

Studies have been made to find the relation between the path and size of water drops as they approach and contact an object in an air stream, and it has been found that as the air-stream velocity and water-drop size increase, the path deflection decreases. Since the resultant velocities of the propeller-blade sections are relatively high and since large water-drop sizes are associated with severe icing conditions, this analysis assumes the deflection of the water drops to be negligible. The weight rate of water striking the blade at any point, or the icing rate, therefore, is a function of the slope of the surface relative to the water-drop path at that point. The rate of icing at any point on the blade can be expressed as a function of the icing rate at the stagnation region. This function is proportional to the slope of the blade-section surface and is termed "R_1." The values of R_1 are measured from the section layouts as shown in figure 1. For sections with flat lower surfaces, R_1 for points on the lower surface is taken to be the sine of the angle of attack measured from the angle of zero lift. For the upper surface, the error due to measuring the slopes from the chord line rather than the relative wind is small and conservative and tends to allow for small changes in α. Each term in equation (15) that expresses the effect of water content must therefore contain the factor R_1 to correct for the slope of the blade-section surface.

The temperature rise at the stagnation point on a propeller-blade section is due to the pressure rise at that point and is

$$T_{A_{stag}} = \frac{V_R^2}{2Jgc_{p_a}} \qquad (16)$$

as noted in reference 10. For any point other than the stagnation point, the temperature rise will be taken to be 0.8 of that at stagnation pressure, or

$$T_A = 0.8\ T_{A_{stag}} \tag{17}$$

The 0.8 factor includes the effects of the laminar and turbulent boundary layers and compressibility, as defined in reference 8, and was approximated from the data of reference 11.

Equation (15), with the effects of aerodynamic heating and blade-surface slope included, becomes at the stagnation-pressure region

$$(q_{bs})_{stag} = h_{stag}\left[32 - T_o - \frac{V_R^2}{2Jgc_{p_a}}\right] + W\left[c_p\ V_R(32 - T_o) - \frac{V_R^3}{2Jg}\right](3600) \tag{18}$$

and at any other point on the blade shoe

$$q_{bs} = h\left[32 - T_o - \frac{0.8\ V_R^2}{2Jgc_{p_a}}\right] + R_i\ W\left[c_p\ V_R(32 - T_o) - \frac{V_R^3}{2Jg}\right](3600) \tag{19}$$

The total heat required at the blade-shoe surface to prevent ice is obtained by the following integration which can best be performed graphically,

$$Q_{bs} = BR\int_{(r/R)_h}^{(r/R)_t}\left[\int_{s_u}^{s_v}(q_{bs})_U\,ds + \int_{s_u}^{s_v}(q_{bs})_L\,ds\right]d\left(\frac{r}{R}\right) \tag{20}$$

where $(r/R)_h$, $(r/R)_t$, s_u, and s_v are the conducting-layer limits of the radial and chordwise extent of the blade shoe.

Heat loss.- In order to provide sufficient heat to maintain the blade-shoe surface at the design temperature, an excess of heat must be supplied to the blade shoe. This excess

of heat represents the heat lost to the atmosphere through the thermal circuit comprised of the blade-shoe insulating layer, the blade material, and the blade-section boundary layer. At any point on the after surface of the propeller blade, the heat loss per unit area q_{as} will be a function of the over-all thermal conductivity of the heat-loss circuit (k/t), the temperature at the point of maximum thermal potential T_2, the ambient-air temperature T_0, and the temperature rise due to aerodynamic heating T_A, and may be expressed as

$$q_{as} = \frac{k}{t} (T_2 - T_0 - T_A) \tag{21}$$

The location of the point of maximum thermal potential in the conducting layer of the blade shoe and the temperature at that point T_2 will be determined by the relative magnitude of the heat transmitted to the blade-shoe surface and the heat lost to the blade. Since T_2 is the maximum temperature which exists in the blade-shoe conducting layer, a decreasing temperature gradient will occur between the location of this point of maximum temperature T_2 and the surface of the insulating layer. The distance through which this decreasing temperature gradient exists in the conducting layer can be considered as an increase in the thickness of the insulating layer. This effective increase in the insulating-layer thickness will be termed Δt_I and is illustrated in figure 1. By assuming the temperature gradients from the point of maximum thermal potential to the blade-shoe surface and to the surface of the insulating layer to decrease linearly with distance, the value of Δt_I can be expressed as

$$\Delta t_I = t_{cl} \left(\frac{Q_{as}}{Q_{as} + Q_{bs}} \right) \tag{22}$$

The value of T_2 can then be determined with sufficient accuracy by the equation

$$T_2 = 32 + \left(q_{bs}\right)_{av} \left(\frac{t_{cl} + \Delta t_I}{k_{cl}} \right) \tag{23}$$

where $\left(q_{bs}\right)_{av}$ is the average value of the unit heat required at the blade-shoe surface at the particular blade

station as determined from the surface heating requirements.

The over-all thermal conductivity of the heat-loss circuit (k/t) can now be defined as a function of its component thermal resistances, the insulating-layer resistance $(t_I + \Delta t_I)/k_I$, the blade-material resistance b/k_b (where b is the chordwise distance through the blade material which the heat is considered to travel), and the boundary-layer resistance $1/h$, or

$$\frac{k}{t} = f\left[\frac{t_I + \Delta t_I}{k_I}, \quad \frac{b}{k_b}, \quad \frac{1}{h}\right] \tag{24}$$

The determination of the thermal loss through a blade element of unit width (fig. 1(a)) can be simplified by assuming certain conservative changes in the heat-loss circuit. The blade-shoe area and the area of the after surface of the blade will be considered to be twice their projected areas or S_{bs} and S_{as}, respectively, while S_b is the projected blade area. The blade-element radial cross-section area S_{cs} is the area of the blade material at any point s_1 through which the heat loss is considered to be conducted and is also shown in figure 1(a). For the purpose of the calculations, the value of S_{cs} can be used more easily by assuming the blade-element material to be a wedge with the base height equal to the maximum blade section thickness t_{max} at the blade station, the base width equal to unity, and the length equal to the chordwise distance from the trailing edge of the conducting layer to the blade trailing edge, as illustrated in figure 1(b). The blade material under the blade shoe is neglected in this heat-loss approximation. The result of these assumptions is an equivalent thermal-loss circuit for each point s_1 on the after surface. As shown in figure 1(c), the heat loss travels from the point of maximum temperature T_s through the effective increase in the insulating-layer thickness Δt_I and then through the insulating-layer thickness t_I to the blade material. Since the material beneath the blade shoe has been neglected, the circuit is represented by considering the blade-shoe layers to be applied to the forward face of the block of blade material of length b, unit width, and thickness t_{cs} as given by the wedge approximation for any point s_1. After the heat has been conducted through the block of blade

material, it is lost to the ambient-air stream by forced convection through the boundary layer. The assumed equivalent heat-loss circuit is complete if the air stream is considered to flow over the opposite end of the block from that which is considered covered by the blade-shoe layers. The complete equivalent heat-loss circuit as described is shown in figure 1(c).

If the unit heat distribution was constant over the blade-shoe surface, the total heat would be given by the equation

$$Q_{as} = \frac{k}{t} S_{as} (T_s - T_o - T_A) \tag{25}$$

But

$$t/k \frac{1}{S_{as}} = \left(\frac{t_I + \Delta t_I}{k_I} \frac{1}{S_{bs}}\right) + \left(\frac{b}{k_b} \frac{1}{S_{cs}}\right) + \left(\frac{1}{h} \frac{1}{S_{as}}\right)$$

where the units of the terms are the reciprocal of Btu per hour, degrees Fahrenheit. The purpose of this step is to express the three factors of the thermal resistance in their proper relation as determined by the different heat-transfer areas for each term. In order that the thermal conductivity k/t can be used for the case of nonuniform heat distribution, or in the expression for q_{as} (equation (21)), the foregoing equation is rearranged as follows:

$$k/t = \frac{1}{\left[\left(\frac{t_I + \Delta t_I}{k_I} \cdot \frac{S_{as}}{S_{bs}}\right) + \left(\frac{b}{k_b} \frac{S_{as}}{S_{cs}}\right) + \frac{1}{h}\right]} \tag{26}$$

therefore, for any point on the blade after surface the unit heat loss can be determined by the equation

$$q_{as} = \frac{T_s - T_o - T_A}{\left[\left(\frac{t_I + \Delta t_I}{k_I} \cdot \frac{S_{as}}{S_{bs}}\right) + \left(\frac{b}{k_b} \cdot \frac{S_{as}}{S_{cs}}\right) + \frac{1}{h}\right]} \tag{27}$$

The total heat loss Q_{as} is obtained by integrating the values of q_{as} over the upper and lower surface of the propeller blade as follows:

$$Q_{as} = BR \int_{(r/R)_h}^{(r/R)_t} \left[\int_{x_v}^{x_w} (q_{as})_U \, dx + \int_{x_v}^{x_w} (q_{as})_L \, dx \right] d(r/R) \quad (28)$$

It has been shown that the evaluation of equation (27) depends on two unknowns Δt_I and T_s which are related. Since Δt_I depends on the relative magnitudes of the heat loss Q_{as} and the heat supplied to the blade shoe Q_{bs}, an initial assumption of Δt_I must be made and checked by solving for Q_{as} and the resulting value of Δt_I used in a second solution for Q_{as} until the values of Δt_I, Q_{as}, and Q_{bs} are in reasonable agreement.

Heat Required for Ice Removal

When the quantity of heat supplied to a propeller blade is reduced below the quantity necessary for ice prevention and ice is allowed to form on the propeller blades, the ice will be thrown off after reaching a certain thickness, which is a function of the power input and power distribution. The insulating quality of the ice allows the blade-shoe surface temperature to rise above 32° F and a water interface to form between the ice and the shoe. The reduction of the adhesion combined with the centrifugal force on the ice due to its mass will result in ice removal.

The process of ice removal can be made to occur at different points and at different intervals, depending on the heat distribution and the local rates of icing and heat transfer. The ice thickness at a point on a blade station can be expressed as a function of the maximum ice thickness, which occurs in the stagnation region, and the rate-of-icing ratio R_1

$$t_1 = t_{1_{stag}} (R_1) \quad (29)$$

If ice is assumed to accumulate on the blade shoe in a smooth continuous layer with no free edges and with the thickness distribution as given by equation (29), the unit heat required for ice removal will be given by the equation

$$q_{bs} = \frac{T_1 - T_o - T_A}{\left[\frac{t_i}{k_i} + \frac{1}{h}\right]} - \frac{W V_R^3 R_i}{2Jg}(3600) \qquad (30)$$

The foregoing equation is analogous to equation (15) except that the effect of the ice layer has been included in the thermal resistance $\left[\frac{t_i}{k_i} + \frac{1}{h}\right]$ and that the second term of equation (15), the heat required to increase the temperature of the air-stream water content to above 32° F, has been omitted. In equation (30) T_1 will have a value of 32° F only for the condition in which a continuous ice layer exists. The second term of equation (30) is the kinetic heating due to the water drops striking the blade and it can be neglected because its omission introduces a small and conservative error. If the term is neglected, the heat required as indicated by

$$q_{bs} = \frac{T_1 - T_o - T_A}{\left[\frac{t_i}{k_i} + \frac{1}{h}\right]} \qquad (31)$$

will not be a function of the water content of the air stream.

In natural icing conditions ice does not form in continuous layers but rather in patches, ridges, or particles. At the edge of a discontinuous ice layer, there will be a heat loss from the iced to the uniced portion of the blade shoe with a temperature gradient along the shoe surface normal to the edge of the ice. (See fig. 4.) If a semi-infinite ice layer is assumed to extend from a point on the blade-shoe surface at which the surface temperature is T_{1_o}, the surface temperature T_1 at any point beneath the ice layer at a distance l from the location of T_{1_o} as a function of the surface temperature at l equals infinity T_{1_∞} is

$$\frac{T_1}{T_{1_\infty}} = 1 - \left[\frac{(1 + T_o/T_{1_\infty})(1 - \psi^2)}{1 + \psi}\right]\left[e^{-\left(\frac{h}{k_{cl}\, t_{cl}}\right)^{\frac{1}{2}} \psi l}\right] \qquad (32)$$

where

$$\psi = \left[\frac{k_i}{k_i + ht_i}\right]^{\frac{1}{3}} \tag{33}$$

which is developed in the appendix and illustrated in figure 4. The ice-thickness parameter ψ expresses the nondimensional relation between the ice thickness t_i and thermal conductivity k_i and the local heat-transfer coefficient h. If a certain size ice particle is assumed to have a negligible effect on the propeller performance, the value of ψ can be determined at any point by using the ice thickness and local value of h in equation (33), the value of the thermal conductivity of ice k_i being a constant. The unit heat required q_{bs} at any point at which ψ is known can be determined by the equation

$$q_{bs} = (T_1 - T_o - T_A)\, h\psi^3 \tag{34}$$

where T_1 is, in this case only, the blade-shoe surface temperature at the center of the smallest surface dimension (2l) of the ice particle when the edge is at 32° F. The use of a unidimensional analysis for a two-dimensional problem is not considered to involve an appreciable error with the size ice particles and values of h normally encountered. The heat required at the blade-shoe surface is obtained by integrating the values of q_{bs} obtained by equation (34) as shown by equation (20), and the heat loss is determined in the same manner as was developed in the ice-prevention section of this report.

A study of equations (32) and (33) indicates that when $\psi = 1$ the ice-particle thickness and surface-temperature gradient are both zero. This indicates that when a water drop strikes the blade shoe, it is immediately thrown off as an ice flake. It is reasoned that there will be some minimum heat requirement for propeller ice removal which will depend on the effect of an ice layer or ice particles on the propeller efficiency and it is possible that the optimum aerodynamic and thermal blade-shoe design will be for the condition of $\psi = 1$.

APPLICATION

It is apparent that in the application of the foregoing method to a specific propeller blade-shoe design, the estimation of the effective angle of attack and resultant velocity at each propeller-blade element is subject to an error due to body interference which will be reflected in the calculation of the heat-transfer coefficients. In addition, it is questionable whether it is judicious to design a propeller blade shoe for a single propeller-operating condition which fixes the blade angle and V/nD. With the foregoing in mind it is suggested that, in a specific design, the method presented herein be repeated over a sufficient range of blade angles and values of V/nD to insure evaluation of the maximum heat-distribution requirements. In this manner a family of chordwise heat-distribution curves for each propeller-blade element is obtained over a safe propeller-operating range, from which family envelope curves can be drawn for all elements to establish the required heat distribution over the entire blade shoe.

In order to illustrate the method developed in this report, sample computations are presented hereinafter on the design of a blade shoe for a Hamilton Standard propeller blade No. 6477A-0. The computations presented are for one propeller-operating condition only and no allowance has been made for body interference. In an actual design, repetition of the method over a selected range of blade angles and values of V/nD, as indicated in the preceding discussion, would be desirable. The Hamilton Standard blade No. 6477A-0 has been selected for the following analysis since this blade was used in the B-17F airplane propellers which were equipped with blade shoes, tested, and reported by the NACA in reference 2. The following flight conditions, for long-range cruising, will be used in the analysis:

Ambient-air temperature, $^{\circ}F$	0
Pressure altitude, ft	10,000
Indicated airspeed, mph	155
Propeller speed, rpm	1012

(For these computations β is assumed to be at the V_0/nD for maximum propeller efficiency.)

These are taken to be the critical conditions for propeller ice protection because the propeller-blade elements are near the maximum practical angle of attack. It is reasoned that the high angle-of-attack condition will result in the maximum heat requirement at the blade-shoe surface because of the decreased extent of the laminar boundary layer on the forward face of the blade.

The area covered by the blade shoe is assumed to extend chordwise to the 20-percent-chord point on both surfaces and from the blade shank at the hub $r/R = 0.145$ to the station at which the tip radius begins $r/R = 0.942$, where $R = 69$ inches. The 20-percent chordwise coverage was satisfactory in the tests reported in reference 2, as was the radial blade-shoe length which extended to $r/R = 0.942$. Actually the radial extent of the blade shoe would be determined by the amount of aerodynamic heating experienced by outer elements of the blade.

The computations follow the same sequence of steps as presented in the section Method.

Determination of the Surface Heat-Transfer Coefficients

The chordwise heat-transfer coefficients were determined at five blade stations (measured in inches from the center of rotation): 21.5, 25.5, 31.5, 42, and 63.5, which correspond to thickness ratios of 0.18, 0.15, 0.12, 0.09, and 0.06. The four outer-blade stations for the 6477A-0 blade were RAF-6 airfoil sections, while the inner section was similar to a modified Clark Y airfoil section.

Propeller-blade section velocity distribution.- The geometric angle of attack α was obtained by calculation of the helix angle Φ and V_o/nD from the flight conditions. The values of θ_M and Φ_M were obtained from figure 10, reference 12. The blade angle θ was obtained from the blade data sheet 157 of reference 12. The geometric blade angle β at 0.75R is given by the approximate relation

$$\beta_{0.75} = \Phi_{0.75} + \theta_M - \Phi_M \qquad (35)$$

By knowing the value of $\beta_{0.75}$, the relation of β to r/R was obtained by

$$\beta = \theta + (\beta_{0.75} - \theta_{0.75}) \tag{36}$$

and α by equation (1). The values of α, β, ϕ, and θ are plotted in figure 5.

The corrections for aspect ratio were made by equations (2) and (3). The angle of zero lift and slope of the section lift curves were obtained from reference 13, and the section lift coefficient for each station was computed using equation (4).

The velocity distribution for the 18-percent-thick section was obtained by the use of the method presented in reference 5. An NACA 0015 airfoil was used as the reference profile because the leading-edge radius was similar to that of the modified section. The velocity distribution over the NACA 0015 airfoil is well defined by experiment. The values of V_r/V_R were obtained as indicated in reference 5 by

$$\frac{V_r}{V_R} = (1 - P_r)^{\frac{1}{2}} \tag{37}$$

where P_r is the P_f of reference 14. The velocity distributions were obtained by adding to this velocity V_r/V_R, the change in velocity $\Delta V/V_R$ due to the difference in shape between the reference profile and the 18-percent-thick section

$$\frac{V_f}{V_R} = \frac{\Delta V}{V_R} + \frac{V_r}{V_R} \tag{38}$$

then

$$\left.\begin{aligned} \frac{V_U}{V_R} &= \frac{V_f}{V_R} + \frac{P/4}{V_f/V_R} \\ \frac{V_L}{V_R} &= \frac{V_f}{V_R} - \frac{P/4}{V_f/V_R} \end{aligned}\right\} \tag{39}$$

where P is the pressure corresponding to the normal force at a chord point given by the equation

$$P_i = P_b + (c_l - c_{l_b})\left(\frac{P_a}{c_{l_a}}\right) \qquad (40)$$

as defined in reference 5. The velocity distribution over the 12-percent-thick RAF-6 blade section was obtained by the method of reference 4 and was modified for the various values of thickness and camber to give the velocity distributions for the remainder of the RAF-6 blade sections. Velocity diftrubutions for the five blade stations are plotted in figures 6 to 10.

Boundary-layer heat transfer.- The chordwise position of the laminar-separation point was determined by approximating the actual velocity distribution by a double-roof profile and finding V_s/V_M from figure 2. The approximate double-roof velocity profiles are shown as dashed lines for the upper and lower surfaces on the velocity-distribution curves in figures 6 to 10. The double-roof profiles are drawn so as to give approximately the same lift (area beneath the curve) up to the laminar-separation point as the velocity-distribution curves. Considerable judgment must be used in the drawing of the profiles in order to obtain reasonable results. Theory indicates that, for the velocity distribution shown in figure 10, laminar separation will not occur on the lower surface of the propeller-blade element. Experience, however, indicates that laminar separation is likely to occur and, since the assumption that separation does occur is conservative, the laminar-separation point shown for the lower surface in figure 10 has been used in this analysis.

The values of boundary-layer thickness and heat-transfer coefficients were computed by equations (6) to (14) and are plotted in figures 6 to 10 with the corresponding velocity distributions. Because of the changes in lift coefficient of the blade sections as the blade angle is changed, the location at which the heat transfer (due to forced convection) approaches zero will move fore and aft from the design position. In order to protect the region of the blade at which low values of h occur at other than design c_l, the curves of h as related to x/c were faired as shown in figure 11 and the faired values were used in succeeding computations.

Heat Required for Ice Prevention

Heat required to maintain the blade-shoe surface at 32° F.- Equations (18) and (19) were used to determine the unit power input to the blade shoes. The water content of the air stream was taken to be 1.84 grams per cubic meter, the maximum water content measured in clouds by Kohler, as described in reference 15.

When the various factors in equations (18) and (19) are fixed by the design conditions, the equations become

$$\left(q_{bs}\right)_{stag} = h_{stag}\left[32 - 0.833 \times 10^{-4} V_R^{2}\right] + 13.1 V_R - 8.18 \times 10^{-6} V_R^{3} \qquad (41)$$

and

$$q_{bs} = h\left[32 - 0.667 \times 10^{-4} V_R^{2}\right] + R_i\left[13.1 V_R - 8.18 \times 10^{-6} V_R^{3}\right] \qquad (42)$$

The heat per unit area required to provide ice protection on the surface of the blade shoe q_{bs} can then be evaluated by substituting in equations (41) and (42) the proper values of h (from fig. 11), R_i, and V_R for the respective point on the blade-shoe surface under consideration. The total heat required at the blade-shoe surface to provide ice protection is obtained by integrating equation (20) over the blade-shoe area, from $r/R = 0.145$ to $r/R = 0.942$ and from s at $x/c = 0$ to $x/c = 0.2$. For the three propeller blades,

$$Q_{bs} = 3R \int_{0.145}^{0.942} \left[\int_{0}^{x/c = 0.2} (q_{bs})_U \, ds + \int_{0}^{x/c = 0.2} (q_{bs})_L \, ds \right] d\left(\frac{r}{R}\right) \qquad (43)$$

The heat required at the blade-shoe surface to provide ice protection was obtained by performing the integration of equation (43) by graphical means. The power required to prevent ice formations on a Hamilton Standard propeller with three No. 6477A-0 blades expressed in electrical units is 3957 watts at the design conditions with the losses through the after portion of the blades neglected. The results of the computations of the unit power distribution are given in figure 12.

Heat loss.- The heat loss from the aft portion of the blade is assumed to occur over the rear 80-percent chord, and from the blade root $r/R = 0.145$ to the tip region $r/R = 0.942$. With these limits, equation (28) becomes

$$Q_{as} = 3R \int_{0.145}^{0.942} \left[\int_{0.2}^{1.0} (q_{as})_U \, dx + \int_{0.2}^{1.0} (q_{as})_L \, dx \right] d\left(\frac{r}{R}\right) \tag{44}$$

The thickness of the outer layer of the blade shoe for this analysis is 0.020 inch or 0.00167 foot, while the inner layer t_I is 0.040 inch or 0.0033 foot thick. At any blade station, the values of S_{bs}/S_b and S_{as}/S_b are taken to be 0.4 and 1.6, respectively (fig. 1); also, from the wedge blade element

$$S_{cs}/S_b = \left(\frac{t}{c}\right)_{max} \left[1 - 1.25 \left(\frac{b}{c}\right)\right] \tag{45}$$

where b is measured from the base of the wedge and $(t/c)_{max}$ is the maximum thickness of the blade section. Therefore, equation (27) becomes

$$(T_s - T_o - T_A) = q_{as} \left[\frac{0.0133 + 4\Delta t_I}{k_I} + \frac{1.6b}{k_b (t/c)_{max} [1 - 1.25\ b/c]} + \frac{1}{h} \right] \tag{46}$$

and when

$$k_I = 0.08 \text{ Btu/hr, ft}^2\text{, }^\circ\text{F/ft}$$

and

$$k_b = 117 \text{ Btu/hr, ft}^2\text{, }^\circ\text{F/ft}$$

then, inserting the foregoing values of thermal conductivity and rearranging the terms, equation (46) becomes

$$q_{as} = \frac{T_s - T_o - T_A}{\left[0.167 + 50\Delta t_I + \frac{0.0137\,b}{(t/c)_{max}[1 - 1.25\,(b/c)]} + \frac{1}{h}\right]} \quad (47)$$

By successive approximations, values of Δt_I, Q_{as}, and Q_{bs} which are in reasonable agreement can be found and the heat loss through the after portion of the propeller can be evaluated by integrating equation (44). A graphical integration of this equation indicates a total heat loss for the entire propeller of 1109 watts.

The total power required to prevent ice formations on a propeller with three 6477A-0 blades with the distribution shown in figure 12 is 3957 + 1109 = 5066 watts.

The calculated power, 5066 watts, is greater than the power used during the flight tests in natural icing conditions reported in reference 2 and is greater than the available power from generators which are now under development for propeller ice prevention. Although the process of ice prevention is probably the ultimate objective in the development of protection for propellers, the process of ice removal as indicated by the results of reference 2 appears to be a practical solution more suitable for immediate application.

Heat Required for Ice Removal

The heat required for ice removal will depend on the maximum size of ice particle that is allowed to form on the propeller blade. Equation (32), when $T_o = 0^\circ$ F and the factor $[1/k_{cl}t_{cl}]^{\frac{1}{2}}$ is evaluated for the particular blade-shoe design, becomes

$$\frac{T_1}{T_{1_\infty}} = 1 - \frac{(1 - \psi^2)}{(1 + \psi)} e^{-100\psi h^{\frac{1}{2}} l} \qquad (48)$$

and since the heat required to remove an ice particle will be a function of the temperature gradient at its edge, the values of T_1/T_{1_∞} for the subject propeller and blade shoe were computed and plotted in figure 13 for various values of ψ^2 and $h^{\frac{1}{2}}l$.

In order to clarify the effect of the surface temperature, an ice particle 0.3 inch in diameter and of variable thickness was assumed to be attached to various points on the blade shoe. The change in air flow over the blade due to the ice particle is assumed to have a negligible effect on the heat transfer. The heat required was based on T_{1_∞} for the various values of ψ^2.

The curves of figure 14 were computed to show the heat required to remove the assumed ice particle as a function of thickness and heat-transfer coefficient. In order to obtain the correct value for the unit power at an ambient-air temperature of 0° F, at any point on the blade, the unit power from figure 14 must be corrected by a function of the aerodynamic heating as shown by the equation

$$(q_{bs})_{correct} = (q_{bs})_{fig.\ 14} - T_A\psi^2 h \qquad (49)$$

With any ice particle of smaller diameter than that assumed, more heat or a greater thickness of ice would be required for its removal. Observations during icing flights have shown that in icing conditions at low temperatures (0° to 10° F), ice forms in a very narrow ridge, sometimes as narrow as 1/4 inch, along the blade leading edge. This condition has been substantiated by other observers (reference 1). The ice which forms at these low temperatures is particularly hard and tenacious. In view of the occurrence of such icing conditions, the use of less heat than that required to maintain the blade-shoe surface at 32° F ($\psi = 1$) in dry air, seems to be inadvisable.

The distribution of the unit power to obtain ice protection by removal at all points on the blade-shoe surface simultaneously, based on figure 14 at $\psi = 1$, is plotted in figure 15. Figure 16 shows the required unit heat distribution on the developed blade-shoe surface.

Graphical integration of the unit heat required over the blade-shoe area gives a value of 1750 watts required to effect ice removal at $\psi = 1$. The heat loss through the after portion of the blade was computed through the use of equations (22), (23), (43), and (44) and was found to be 640 watts. The total power required for ice protection by the removal process at $\psi = 1$ is therefore 2390 watts.

DISCUSSION

Benefits Obtained from the Optimum Heat Distribution

In view of the relative simplicity of construction of a propeller-blade shoe with a stepped type of heat distribution, such as was used in the tests reported in reference 2, when compared with a blade shoe having an optimum heat distribution as shown in figure 16, it is important that the blade-shoe designer realize the benefits which may be expected by utilizing a blade shoe having an optimum heat distribution. To indicate the advantages of an optimum heat distribution, the method of analysis developed in this report has been employed to compare the amount of power required by the two types of distribution to provide the same degree of ice protection and to determine the thickness of ice which would be built up upon a blade shoe with a stepped heat distribution utilizing a power input equal to that required for complete ice removal on a blade shoe with an optimum heat distribution. In this comparison the optimum heat distribution shown in figure 16 has been compared with a stepped heat distribution in which the distribution over the leading-edge third of the blade shoe is double that over the remaining area. The chordwise heat distribution for the blade shoe with the stepped distribution has been considered constant over the radial extent of the blade shoe and has been based upon the point of maximum heat requirement for the blade-shoe surface. The chordwise distribution for each type of heat distribution is shown in figure 17 at the critical propeller station.

The calculated total heat required for the distribution shown in figure 16 at $T_0 = 0^\circ$ F and $\psi = 1$ is 2390 watts, while the calculated power required for the stepped distribution, based on the point of maximum heat requirement on the blade-shoe surface (station 42 stagnation region) at the same conditions, is approximately 4800 watts. To enable a

comparison with the experimental results, the heat required by the optimum distribution and the stepped distribution were computed for the test conditions. These conditions were comparable to those listed under the section of this report designated Application, except for the ambient-air temperature which was 10° F instead of 0° F. The computations indicate that 1640 watts are required by the optimum distribution and approximately 3300 watts by the stepped distribution (both at $\psi = 1$). The use of an optimum heat distribution rather than the stepped distribution should, therefore, reduce the total heat required by approximately one-half for the same degree of protection against ice formation. Lacking more extensive experimental confirmation, the absolute magnitude of the foregoing power requirements are subject to some doubt; however, their relative magnitude should be reliable.

If the stepped heat distribution is used, but with a power input of 2390 watts at the flight conditions listed, ice will accumulate until its thickness supplies sufficient insulation for the removal process to take place. Application of the foregoing method to compute this thickness indicates that an ice cap 3.42 inches high by 0.3 inch wide (width assumed, based on observations) would form before being removed by melting at the base. Obviously, such an ice structure would be unstable and break, leaving the leading edge with a rough, broken ice cap and, thus, the blade shoe would fail in its function of ice removal.

Comparison with Experiment

The foregoing deductions must be qualified and consideration must be given to the lack of experimental verification of the proposed method. Such experimental verification is particularly needed because of the assumptions which were necessary in the development of the computation procedure. The results of reference 2 are the only experimental data that can be compared with the analytical results. These tests indicated that satisfactory ice-removal characteristics would be obtained with 2100 watts applied to the stepped distribution of the blade shoes tested (ψ not known), while the computations indicate that approximately 3300 watts will be required with the same distribution at similar conditions ($\psi = 1$). In view of this lack of agreement, a critical view of the assumptions upon which the method is based is in order.

Review of Assumptions

As the method was applied, two assumptions appear to be conservative. In the first place, body interference was neglected, which eliminates from consideration the blocking of the air and the resultant reduced velocity over the region of the propeller close to the shank. Data are available which indicate that, on an air-cooled nacelle-propeller combination of the same general dimensions as that on the B-17F airplane, the axial velocity is approximately free stream from the tip to the 0.5 r/R station and then decreases linearly to approximately one-half free-stream velocity at the 0.2 r/R station. A reduction in the computed heat requirements for the inner-blade sections would obviously occur if allowance were made for the reduced velocity.

A secondary result of the reduced axial velocity will be an increased effective blade angle over the inner stations. The magnitude or direction of the deviation requlting from this difference is difficult to predict, but these blade sections will carry a higher lift coefficient than that assumed. By reference to figures 6, 7, and 8, it can be reasoned that this will cause an increased peak velocity on the upper surface, thus decreasing the extent of laminar flow, but will have a compensating effect on the lower surface where the peak will tend to be lowered. Which of these changes will predominate could only be determined by a detailed calculation.

A second conservative assumption is the neglect of centrifugal-force effects. This was justified originally on the basis of the possibility of a reasonably uniform glaze-ice layer formed from the maximum possible water content of the air stream at an ambient-air temperature of 0° F. Under these conditions, the adhesion of ice to the blade-shoe material is greater than the strength of the ice itself. That this assumption may be unduly rigorous can be deduced from the result of reference 2, which indicated the possibility that no heat at all might be necessary to de-ice the outer portion of the blade. Whether this is due to aerodynamic heating or centrifugal-force effects is difficult to determine. However, the basis for the computations of the aerodynamic heating is reasonably sound, while the possibility definitely exists that an ice formation more porous than the glaze ice assumed would adhere less strongly and, therefore, be thrown off by centrifugal force; also, the porosity of this ice layer should have a marked effect on its thermal

resistance. No answer to these possibilities can be proposed without further study.

Several unconservative assumptions were made in the analysis which would tend to cancel the error caused by the neglect of body interference and centrifugal force. The more important of these is the assumption that transition will occur by the process of separation in the adverse pressure gradient. Actually if any ice forms around the leading edge, it is likely to cause local peak pressures or, through roughness, promote earlier transitions. Thus, instead of the fairly extensive laminar flow over the upper surface, turbulent flow might be present. Since the accuracy of the method is largely dependent on the computed location of boundary-layer transition, this would have an important influence tending to make the method unconservative. For ice accumulations occurring with ice removal at ψ of less than 1, the actual formation of ice layers and ice flecks will vary widely over the blade and will tend to increase turbulence further and to effect the rate of heat transfer.

The effects of humidity, evaporation, and degree of supercooling of the water drops have also been neglected; however, these effects are considered to be sufficiently small as to be compensated by other conservative assumptions.

Recommendations

The quantity of power required for ice prevention (5066 watts) appears to be prohibitive at the present stage of development. Because of the weight of the hub generator that would be required, the advantage of the lighter weight of the thermal-electric system in comparison with other methods would be lost. The most expedient present solution appears to be a design for ice removal at ψ equal to 1. If advantage is taken of the reduction in heat requirements made possible by use of an optimum heat distribution, and if the thickness of the conducting layer is kept to a minimum to reduce the heat lost through the after surface of the blade, a blade shoe which will provide satisfactory ice protection with available hub generators should result. In order to obtain the required heat distribution with a satisfactorily thin conducting layer, a material of varying electrical resistance, but constant thickness, would be advantageous.

As a result of limited tests, it has been found that present conducting materials do not have satisfactory

resistance to abrasion and wear. It has been thought that a thin layer of nonconducting rubber over the entire blade-shoe surface would provide the abrasion resistance necessary for satisfactory service life. The effect of the addition of a protective layer can be determined by including its thickness in the thickness of the conducting layer.

Ames Aeronautical Laboratory,
National Advisory Committee for Aeronautics,
Moffett Field, Calif.

REFERENCES

1. Orr, J. L.: Interim Report on Flight Tests of Thermal-Electric Propeller De-Icing. Rep. No. MD-25, Nat. Research Council of Canada, Nov. 7, 1942.

2. Scherrer, Richard, and Rodert, Lewis A.: Tests of Thermal-Electric De-Icing Equipment for Propellers. NACA ARR No. 4A20, 1944.

3. Durand, William Frederick, Ed.: Aerodynamic Theory. Vol. IV. J. Springer (Berlin), 1934.

4. Theodorsen, T., and Garrick, I. E.: General Potential Theory of Arbitrary Wing Sections. NACA Rep. No. 452, 1933.

5. Allen, H. Julian: General Theory of Airfoil Sections Having Arbitrary Shape or Pressure Distribution. NACA ACR No. 3G29, 1943.

6. von Kármán, Th., and Millikan, C. B.: On the Theory of Laminar Boundary Layers Involving Separation. NACA Rep. No. 504, 1934.

7. Allen, H. Julian, and Look, Bonne C.: A Method for Calculating Heat Transfer in the Laminar Flow Region of Bodies. NACA RB, Dec. 1942.

8. Frick, Charles W., Jr., and McCullough, George B.: A Method for Determining the Rate of Heat Transfer from a Wing or Streamline Body. NACA ACR, Dec. 1942. (Classification changed to "Restricted," Aug. 1943)

9. Nitzberg, Gerald E.: A Concise Theoretical Method for Profile-Drag Calculation. NACA ACR No. 4B05, 1944.

10. Rodert, Lewis A.: The Effects of Aerodynamic Heating on Ice Formations on Airplane Propellers. NACA TN No. 799, 1941.

11. Brun, Edmond: Distribution of Temperatures over an Airplane Wing with Reference to the Phenomena of Ice Formation. NACA TM No. 883, 1938.

12. Anon.: Hamilton Standard Method of Propeller Performance Calculation. Hamilton Standard Propellers, Div. of United Aircraft Corp., 1941.

13. Weick, Fred E.: Aircraft Propeller Design. McGraw-Hill Book Co., Inc., 1930.

14. Allen, H. Julian: A Simplified Method for the Calculation of Airfoil Pressure Distribution. NACA TN No. 708, 1939.

15. French Committee for the Study of Ice Formation: Report on Ice Formation on Aircraft. NACA TM No. 919, 1939.

APPENDIX

An expression for the temperature gradient in the edge of an ice layer is to be developed for determining the size and thickness of an ice particle that will adhere to a blade-shoe surface with different unit power inputs. In the derivation of this expression symbols will be used which do not appear in the nomenclature of this report (C_1, C_2, f, u, and v). It was felt that better continuity and clarity could be had by defining the symbols as they appear.

The diagrams of figure 4 illustrate a section through the propeller blade normal to the edge of an ice layer and the temperature profile.

From $l = 0$ to $l = \infty$, the extent of the ice layer,

$$Q_l + dQ_{m_2} = dQ_{m_1} + Q_l - dQ_l$$

then simplifying and dividing by dl gives

$$\frac{dQ_l}{dl} = \frac{dQ_{m_1}}{dl} - \frac{dQ_{m_2}}{dl}$$

Furthermore

$$Q_l = k_{cl} t_{cl} \frac{dT_l}{dl}$$

and differentiating gives

$$\frac{dQ_l}{dl} = k_{cl} t_{cl} \frac{d^2 T_l}{dl^2}$$

When the power input is considered to supply Q_{m_2} then

$$dQ_{m_2} = q_{bs}\, dl$$

and from figure 4

$$dQ_{m_1} = \left[\frac{T_l - T_o}{\frac{l}{h} + \frac{t_i}{k_i}} \right] dl$$

Substitution gives the equation

$$k_{cl} t_{cl} \frac{d^2 T_l}{dl^2} = \frac{T_l - T_o}{\frac{l}{h} + \frac{t_i}{k_i}} - q_{bs}$$

Dividing through by $(k_{cl} t_{cl})$ the equation takes the form

$$\frac{d^2 T_l}{dl^2} = u^2 (T_l - T_o) - v$$

where

$$u = \left[\frac{hk_1}{k_1 + ht_1} \frac{1}{k_{cl} t_{cl}} \right]^{\frac{1}{2}}$$

$$v = \frac{q_{bs}}{k_{cl} t_{cl}}$$

If

$$f = (T_1 - T_0)$$

then

$$\frac{d^2 f}{dl^2} = u^2 f - v$$

The solution of this equation is of the form

$$f = C_1 e^{ul} + C_2 e^{-ul} + \frac{v}{u^2}$$

where C_1 and C_2 are constants of integration and

$$\frac{v}{u^2} = q_{bs} \frac{k_1 + ht_1}{hk_1} = T_{1_\infty} - T_0$$

Substitution gives

$$T_1 - T_0 = C_1 e^{ul} + C_2 e^{-ul} + (T_{1_\infty} - T_0)$$

and when l becomes large $(T_1 - T_0)$ approaches a finite value asymptotically as indicated in figure 4. Therefore,

$$C_1 = 0$$

and

$$T_1 = C_2 e^{-ul} + T_{1_\infty}$$

When l approaches zero

$$T_{1_0} = C_2 + T_{1_\infty}$$

Similarly, the equation for the surface temperature from $l = 0$ to $-\infty$ takes the form

$$k_{cl}t_{cl}\frac{d^2T_1}{dl^2} = h(T_1 - T_0) - q_{bs}$$

and

$$T_1 = C_1e^{ul} + T_{1_{-\infty}}$$

where

$$u = \left[\frac{h}{k_{cl}t_{cl}}\right]^{\frac{1}{2}}$$

At $l = 0$

$$T_{1_0} = C_1 + T_{1_{-\infty}} = C_2 + T_{1_\infty}$$

and

$$C_1 = C_2 + T_{1_\infty} - T_{1_{-\infty}}$$

Also, when the subscripts + and - are introduced to indicate positive and negative values of l,

$$\frac{dT_{1_+}}{dl} = -u_+C_2e^{-u_+l}$$

and

$$\frac{dT_{1_-}}{dl} = u_-C_1{}^{u_-l}$$

When l equals zero,

$$\frac{dT_{1_+}}{dl} = -u_+C_2$$

and

$$\frac{dT_{1_-}}{dl} = u_-C_1$$

Equating the two foregoing equations and substituting the value for C_1 result in the expression

$$-u_+ C_2 = u_-(C_2 + T_{1_\infty} - T_{1_{-\infty}})$$

and, rearranging terms,

$$C_2 = -\frac{T_{1_\infty} - T_{1_{-\infty}}}{\left[\frac{u_+}{u_-} + 1\right]}$$

Substitution of the equation for C_2 in the equation for T_1, for $l = 0$ to $l = \infty$, results in the expression

$$T_1 = T_{1_\infty} - \frac{T_{1_\infty} - T_{1_{-\infty}}}{\frac{u_+}{u_-} + 1} e^{-ul}$$

Because q_{bs} is uniform over the element of blade surface being considered,

$$h\,(T_{1_{-\infty}} - T_o) = \frac{k_i h}{k_i + ht_i}(T_{1_\infty} - T_o)$$

or

$$T_{1_{-\infty}} = \frac{k_i}{k_i + ht_i}(T_{1_\infty} - T_o) + T_o$$

and, making the final substitutions in the expression for T_1

$$T_1 = T_{1_\infty} - \frac{T_{1_\infty} - \frac{k_i}{k_i + ht_i}(T_{1_\infty} - T_o) + T_o}{\left[\frac{k_i}{k_i + ht_i}\right]^{\frac{1}{2}} + 1} e^{-\left[\frac{hk_i}{k_i + ht_i}\frac{1}{k_{cl}t_{cl}}\right]^{\frac{1}{2}} l}$$

Introducing the ice-thickness parameter

$$\psi^2 = \left[\frac{k_i}{k_i + ht_i}\right]$$

the foregoing equation may be written in the form

$$T_1 = T_{1_\infty} - \left[\frac{T_{1_\infty} - \psi^2 (T_{1_\infty} - T_0) + T_0}{\psi + 1}\right]\left[e^{-\left(\frac{1}{k_{c1} t_{c1}}\right)^{\frac{1}{2}} \psi h^{\frac{1}{2}} l}\right]$$

or

$$\frac{T_1}{T_{1_\infty}} = 1 - \left[\frac{\left(1 + \frac{T_0}{T_{1_\infty}}\right)\left(1 - \psi^2\right)}{\psi + 1}\right] e^{-\left[\frac{1}{k_{c1} t_{c1}}\right]^{\frac{1}{2}} \psi h^{\frac{1}{2}} l}$$

and when $T_0 = 0$

$$\frac{T_1}{T_{1_\infty}} = 1 - \left[\frac{1 - \psi^2}{1 + \psi}\right] e^{-\left[\frac{1}{k_{c1} t_{c1}}\right]^{\frac{1}{2}} \psi h^{\frac{1}{2}} l}$$

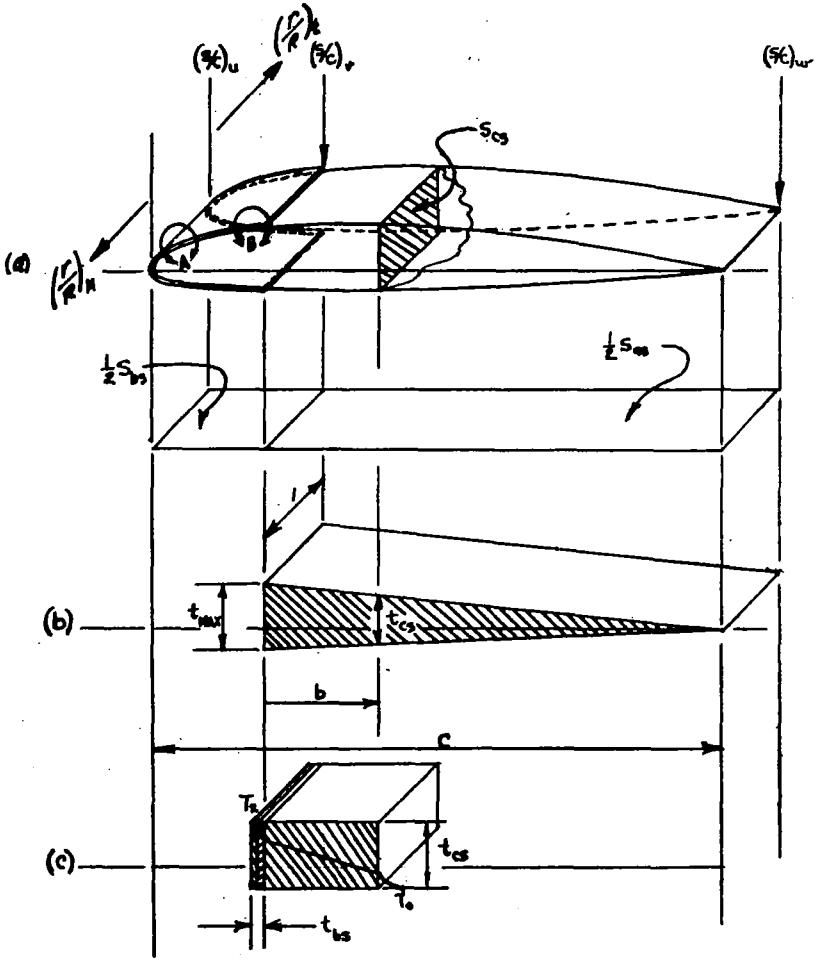

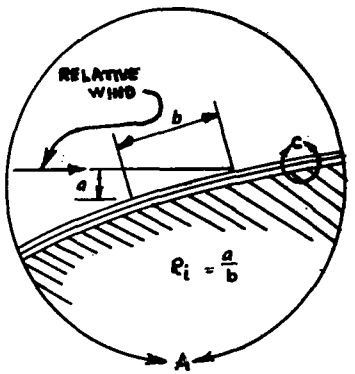

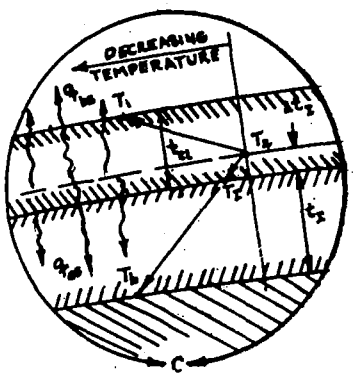

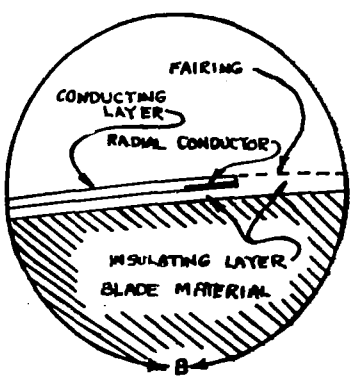

NATIONAL ADVISORY COMMITTEE FOR AERONAUTICS

FIGURE 1.— BLADE-SHOE AND BLADE-ELEMENT DETAILS

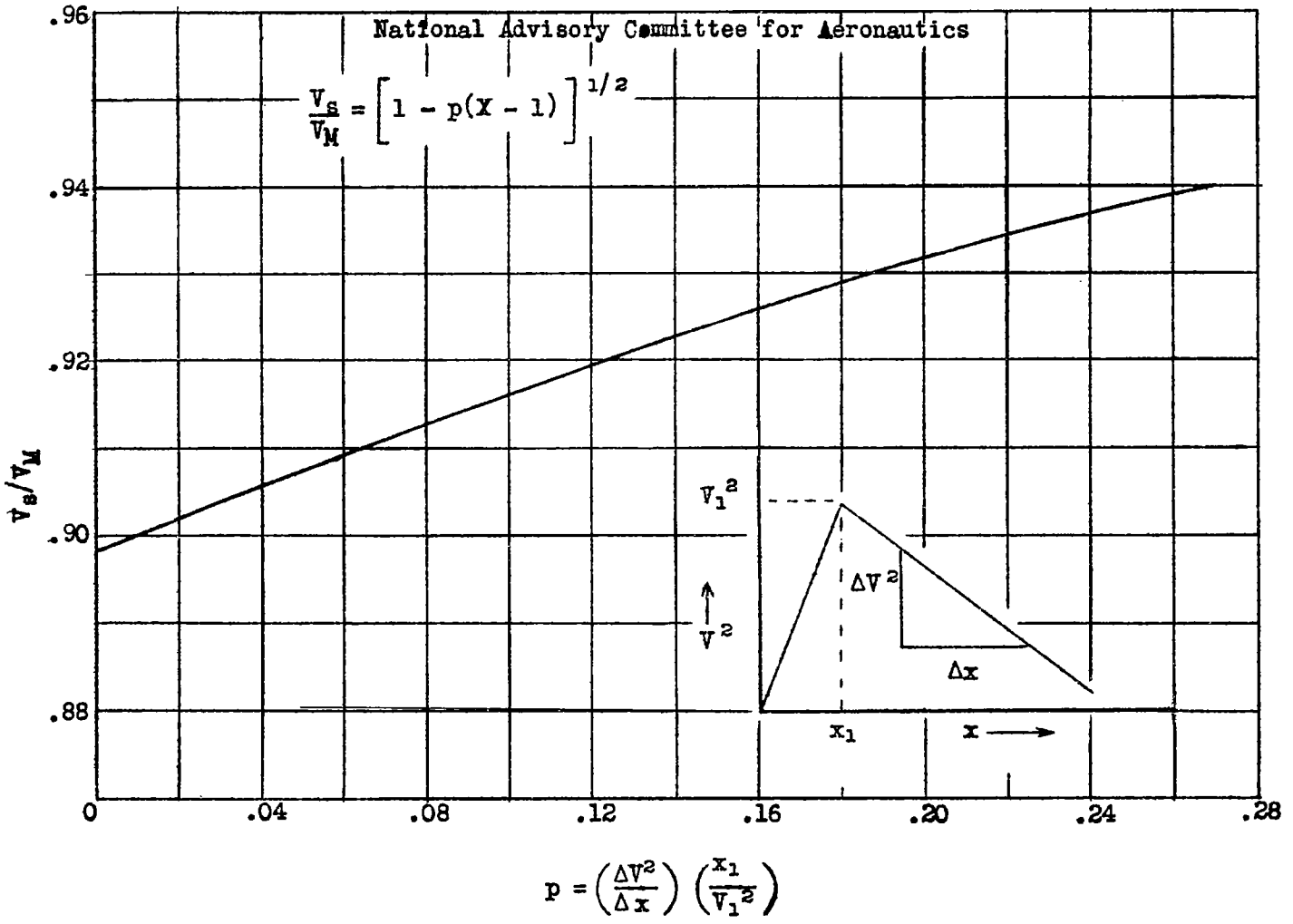

Figure 2.- The ratio of the local velocity at laminar separation, V_s, to the maximum local velocity, V_M, as a function of the ratio of the slopes of the double-roof velocity profile, p.

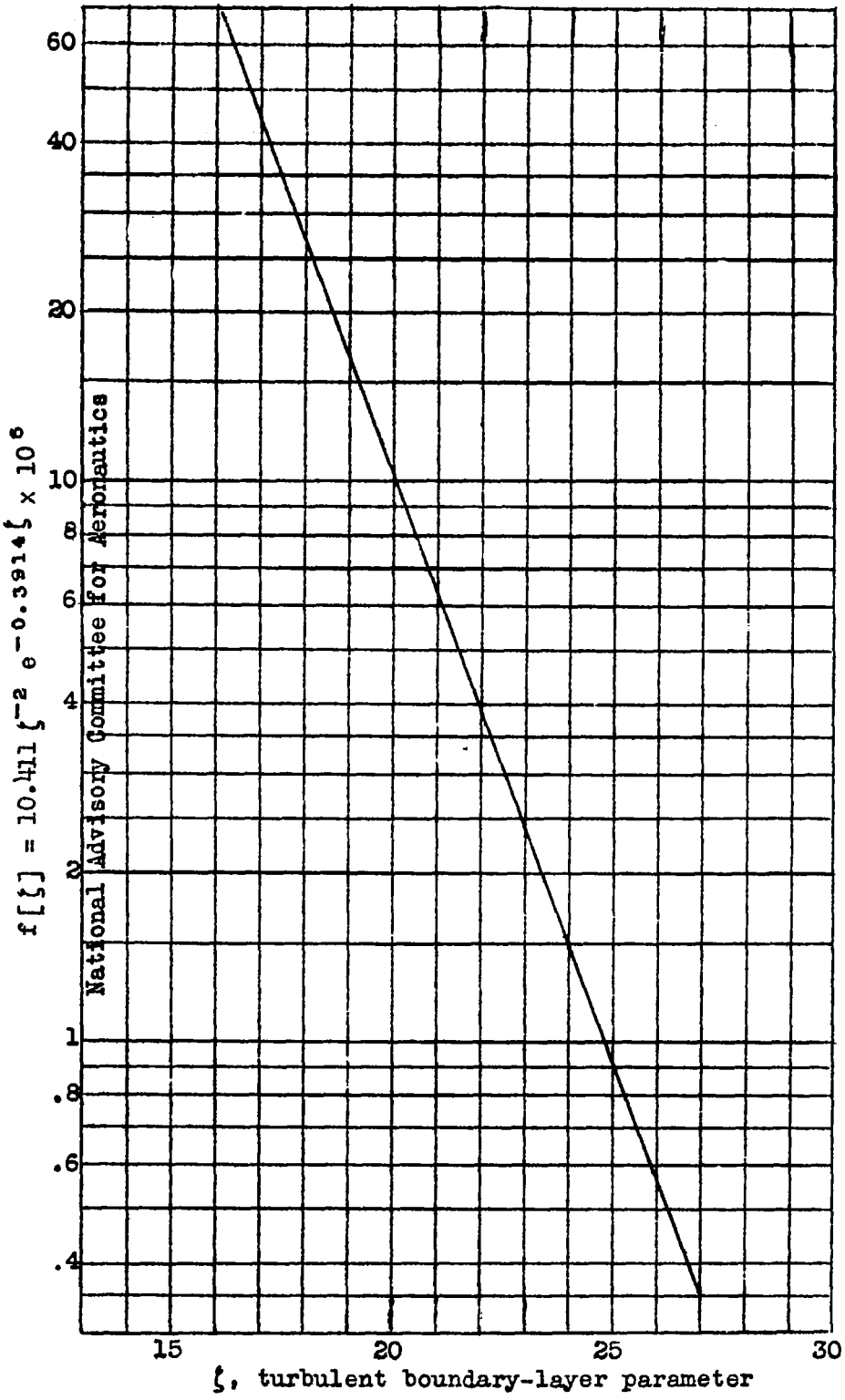

Figure 3.- Variation of $f[\zeta]$ with ζ for the turbulent boundary-layer thickness calculations.

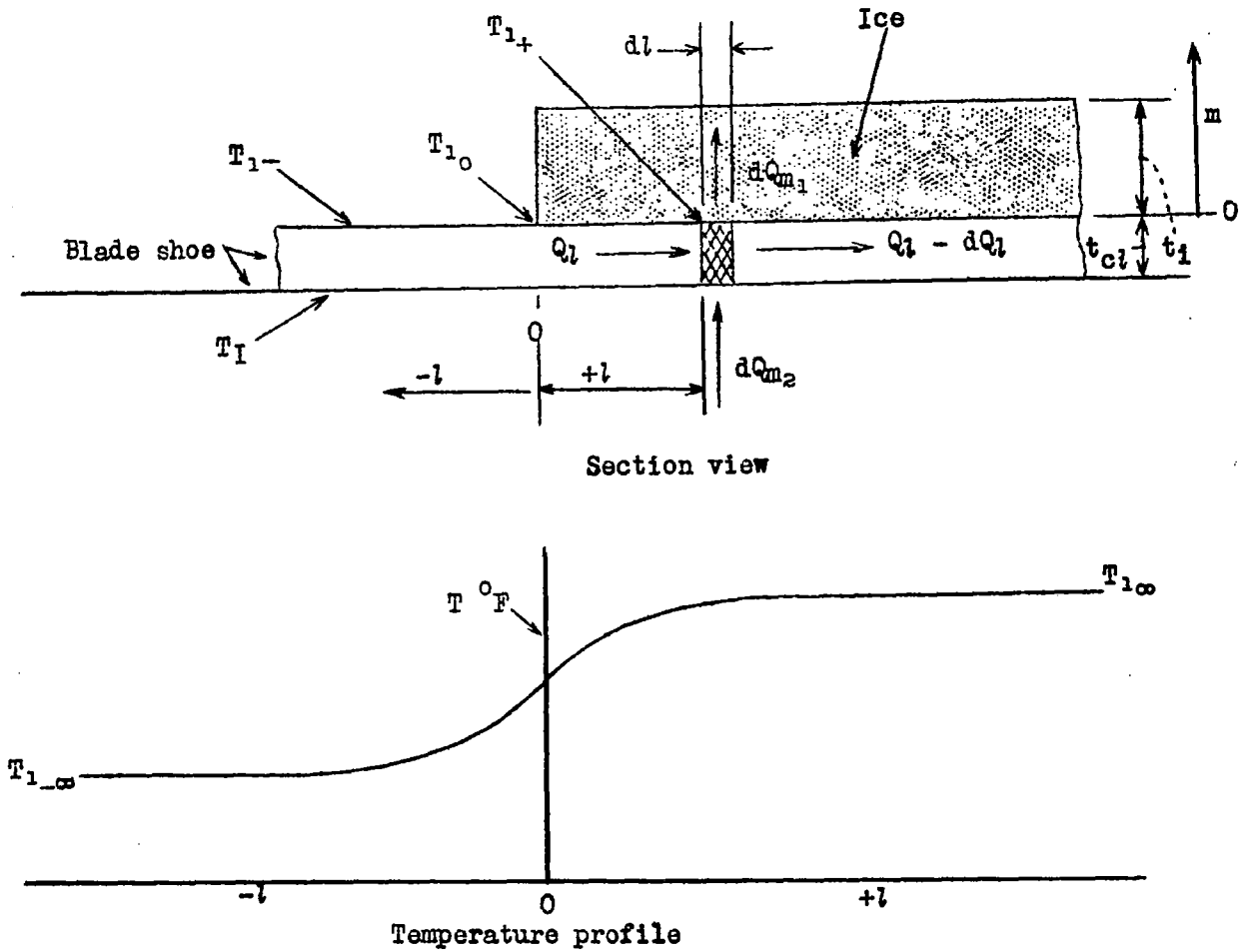

Figure 4.- A section view and temperature profile normal to the edge of an ice layer.

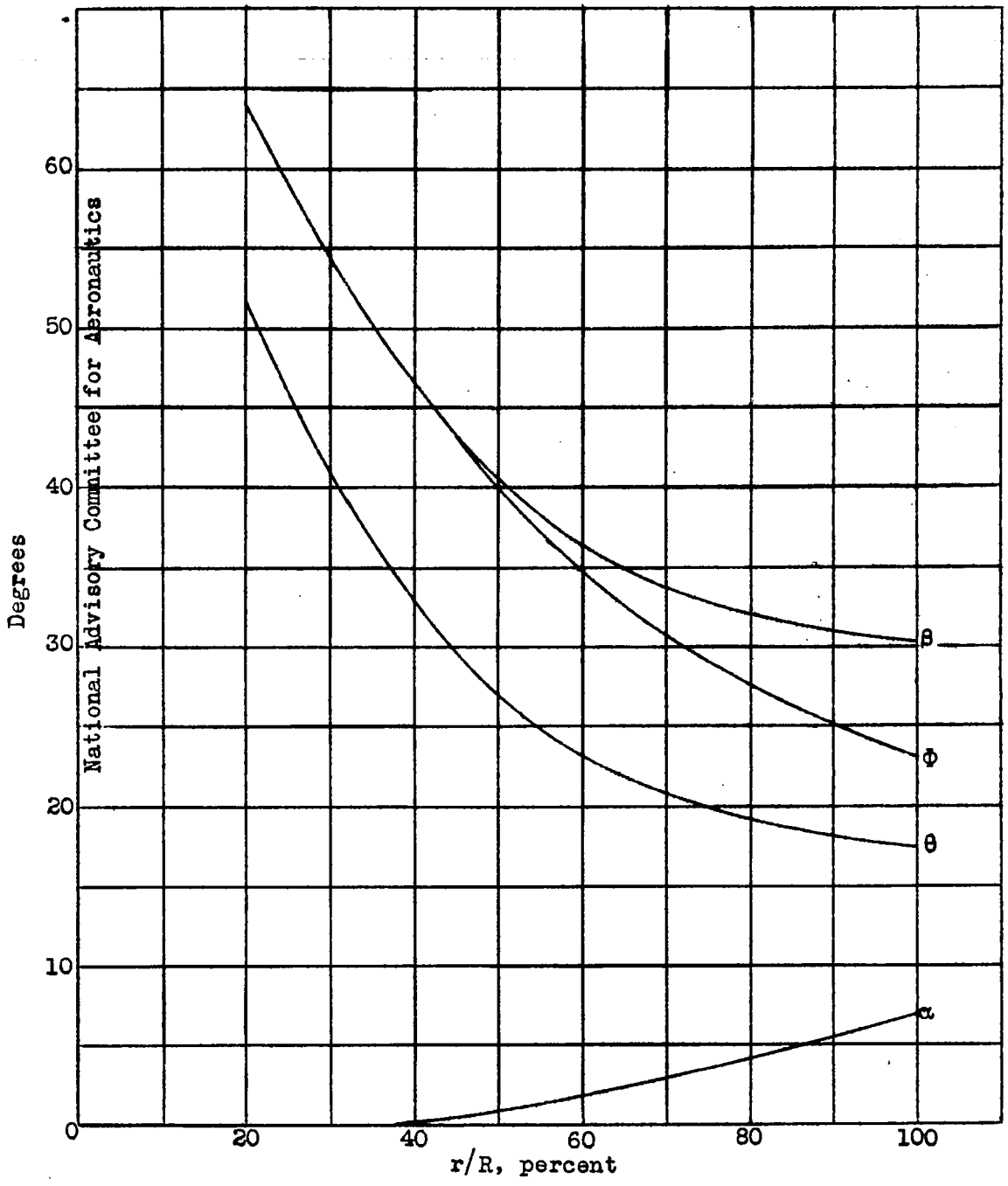

Figure 5.- Variation of propeller-blade angle, β, helix angle, Φ, blade-angle distribution, θ, and angle of attack, α, with percent radius for the Hamilton Standard blade No. 6477A-0 at the design conditions.

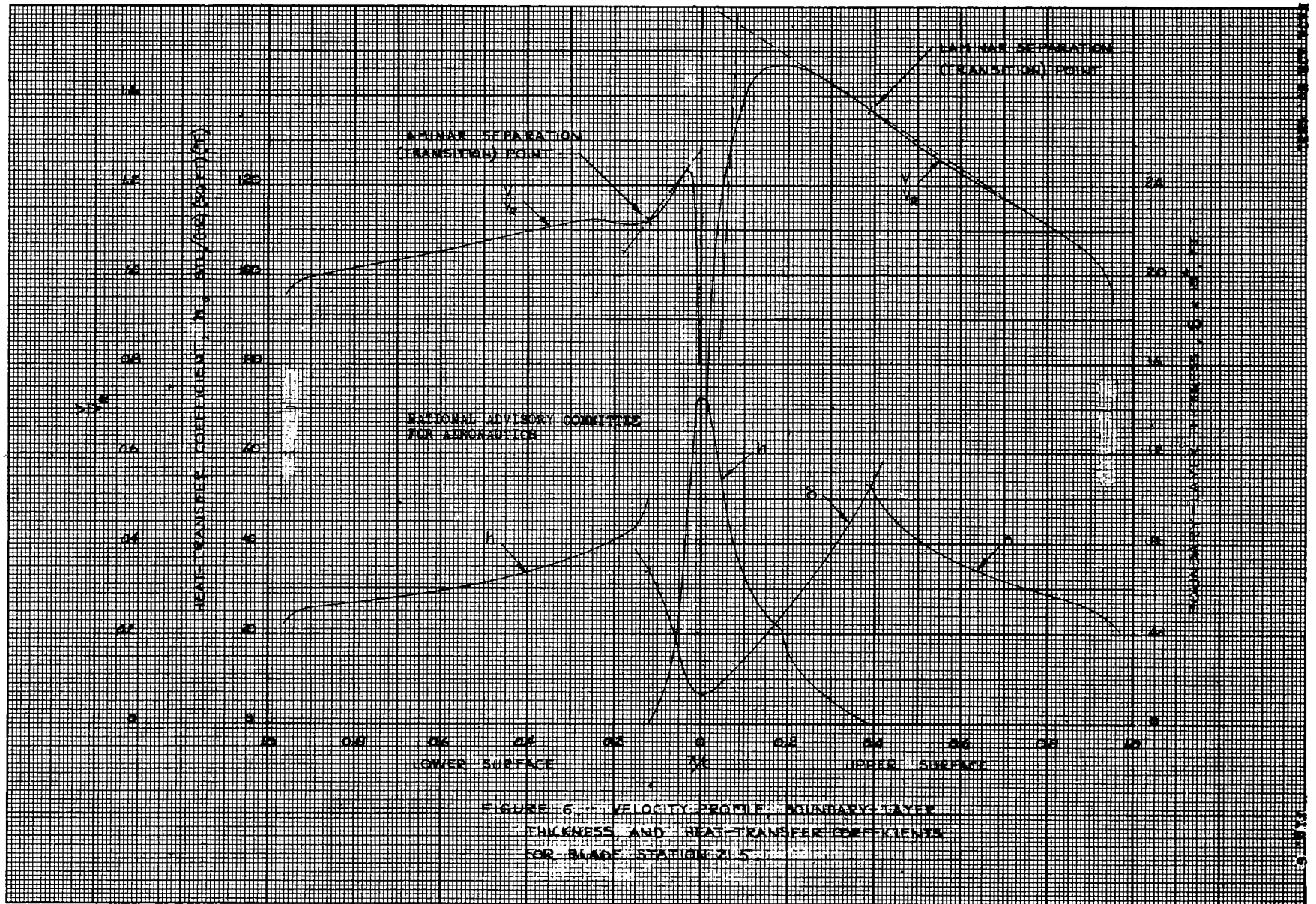

FIGURE 6.- VELOCITY PROFILE, BOUNDARY-LAYER THICKNESS, AND HEAT-TRANSFER COEFFICIENTS FOR BLADE STATION 21.5.

PRINTED IN U.S.A.

EUGENE DIETZGEN CO., CHICAGO-NEW-YORK NO. 346 B

Fig. 7

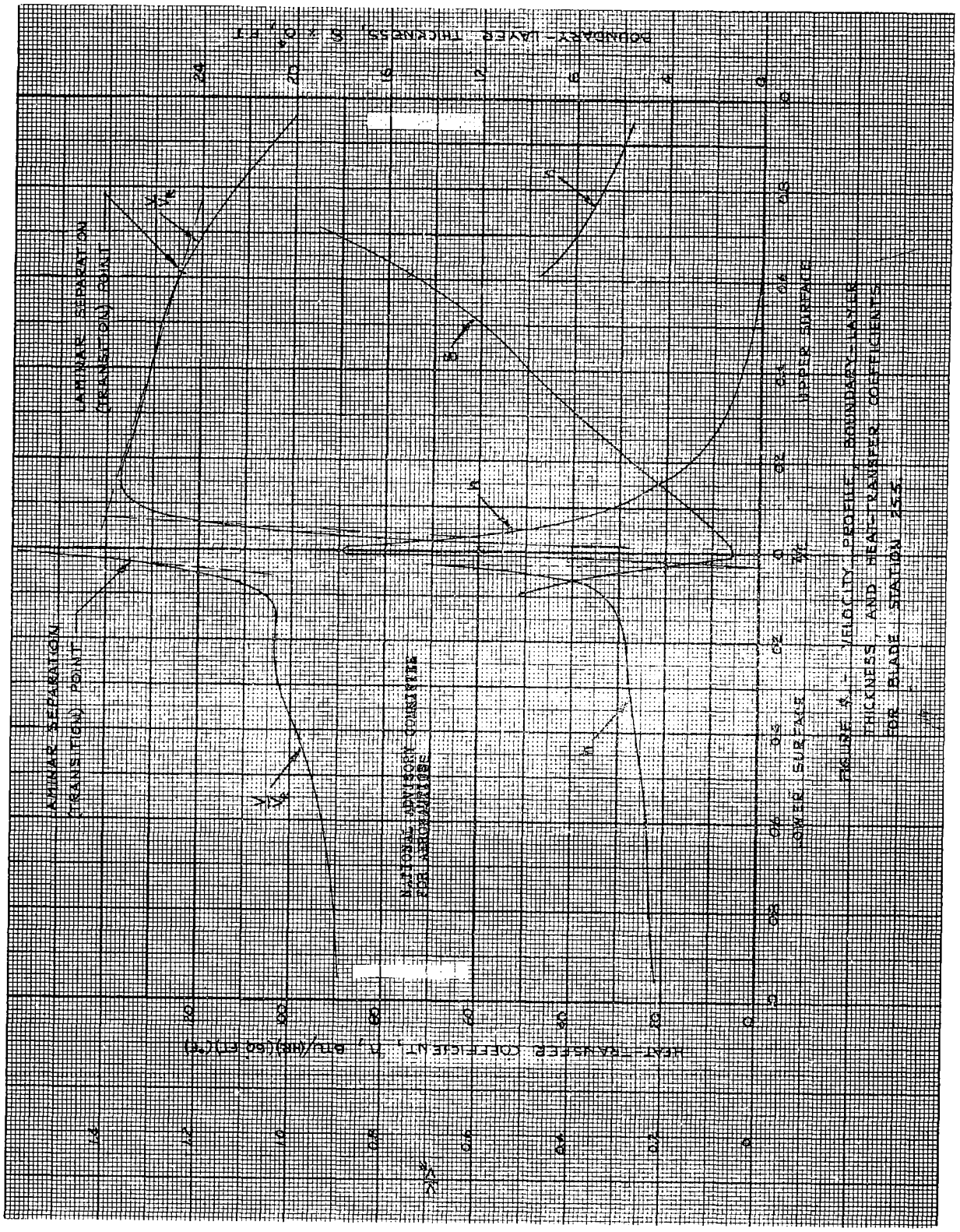

FIGURE 7.- VELOCITY-PROFILE, BOUNDARY-LAYER THICKNESS, AND HEAT-TRANSFER COEFFICIENTS FOR BLADE STATION 25.

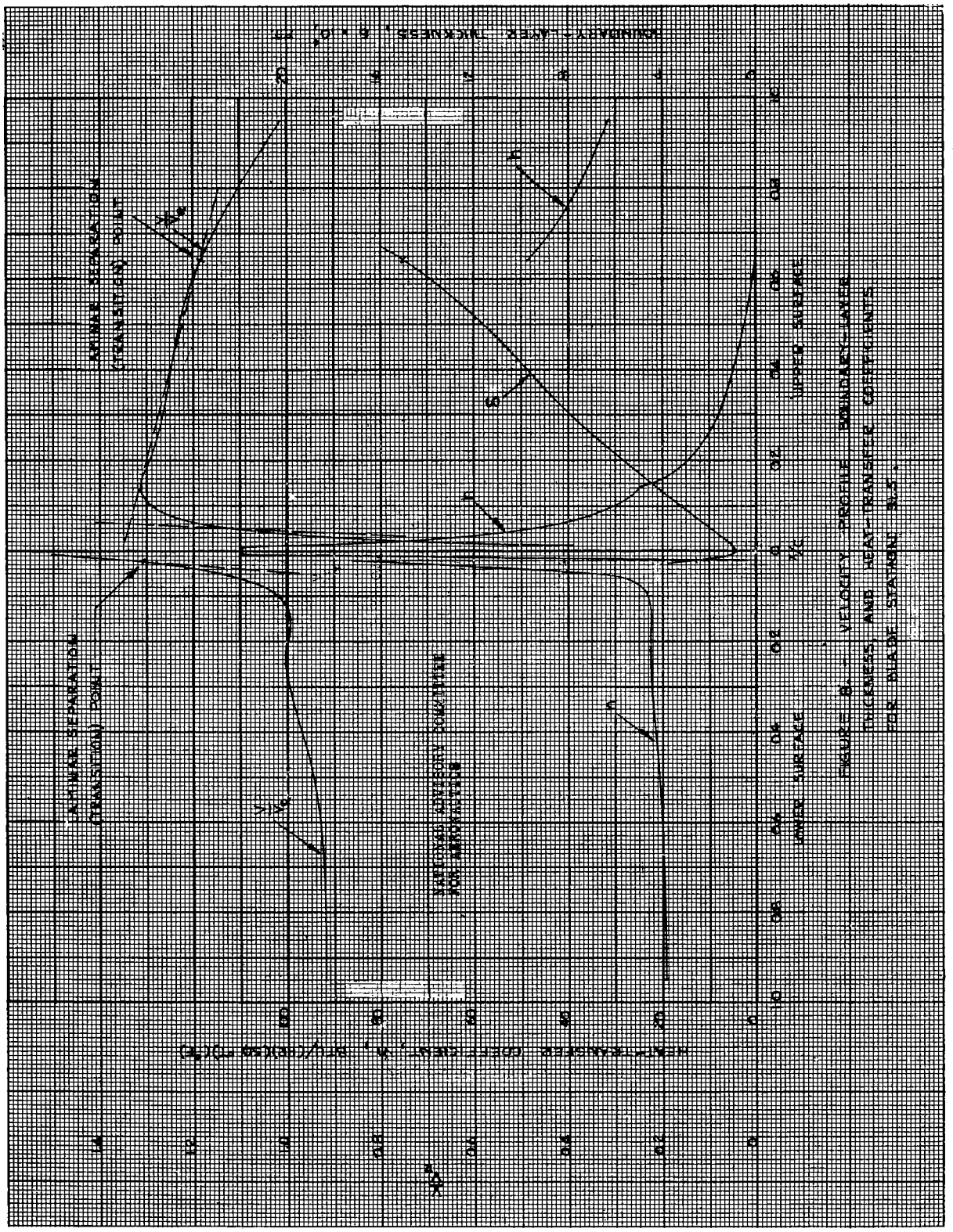
BOUNDARY - LAYER THICKNESS, δ, IN.
LOCAL HEAT-TRANSFER COEFFICIENT, h, BTU/(HR)(SQ FT)(°R)
LAMINAR SEPARATION (TRANSITION) POINT
TURBULENT SEPARATION POINT
LAMINAR
TRANSITION
TURBULENT
LOCAL MACH NUMBER
FIGURE 8 - VELOCITY PROFILE BOUNDARY-LAYER THICKNESS, AND HEAT-TRANSFER COEFFICIENTS FOR A FLAT STANDARD 6% AIRFOIL

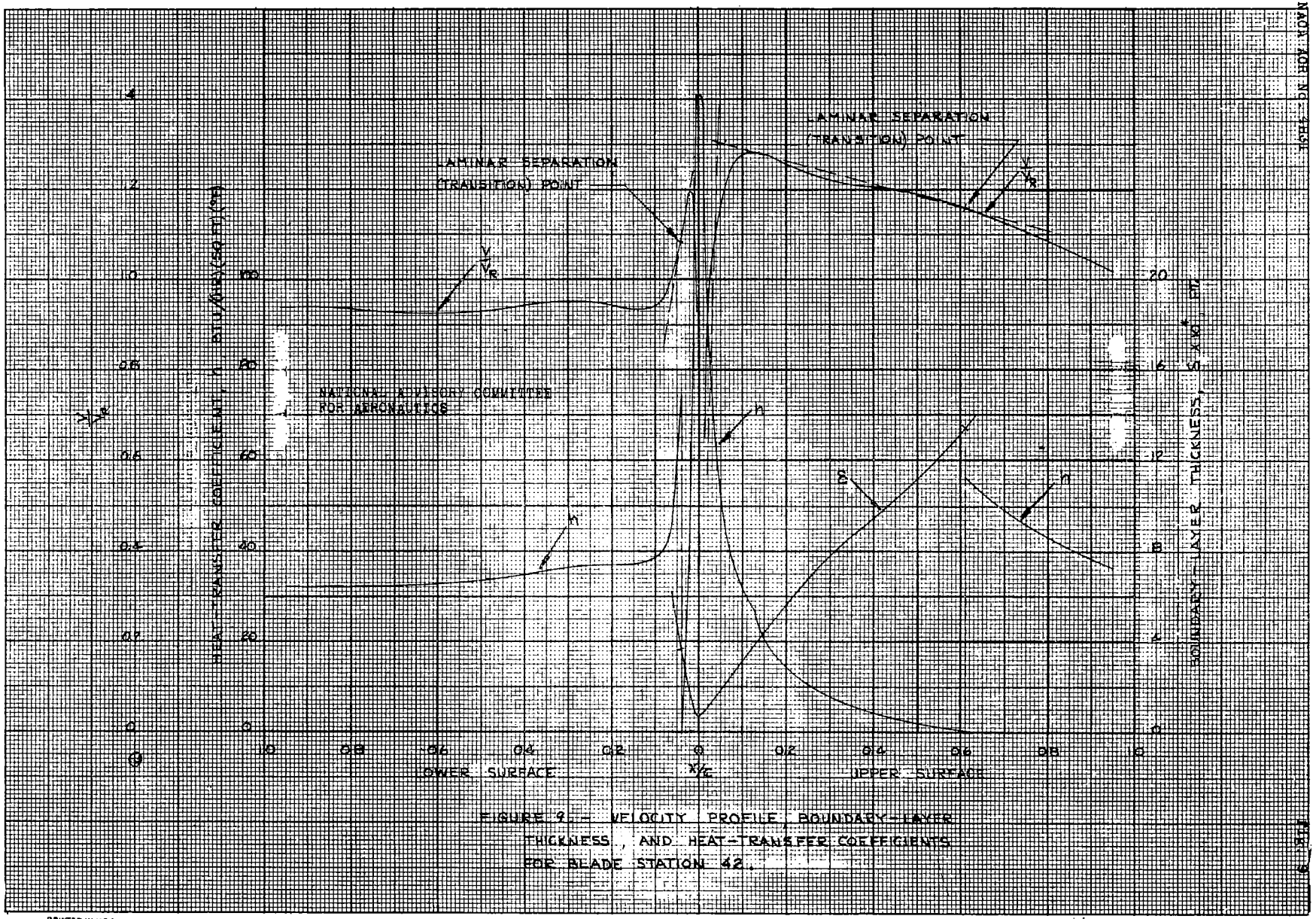

FIGURE 9.— VELOCITY PROFILE, BOUNDARY-LAYER THICKNESS, AND HEAT-TRANSFER COEFFICIENTS FOR BLADE STATION 42.

FIGURE 10.— VELOCITY PROFILE, BOUNDARY-LAYER THICKNESS, AND HEAT-TRANSFER COEFFICIENTS FOR BLADE STATION AT 45%.

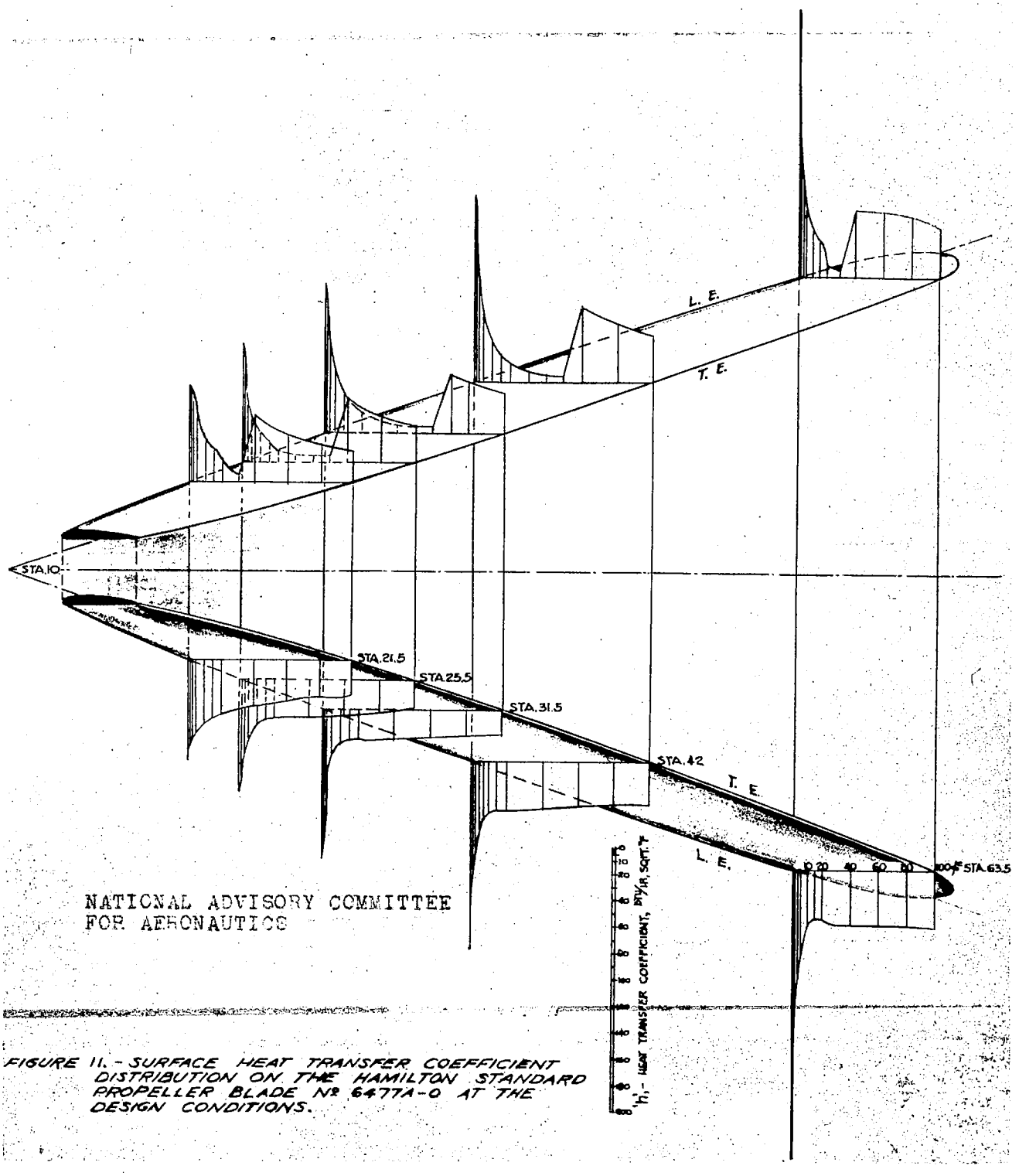

FIGURE 11. - SURFACE HEAT TRANSFER COEFFICIENT DISTRIBUTION ON THE HAMILTON STANDARD PROPELLER BLADE No 6477A-0 AT THE DESIGN CONDITIONS.

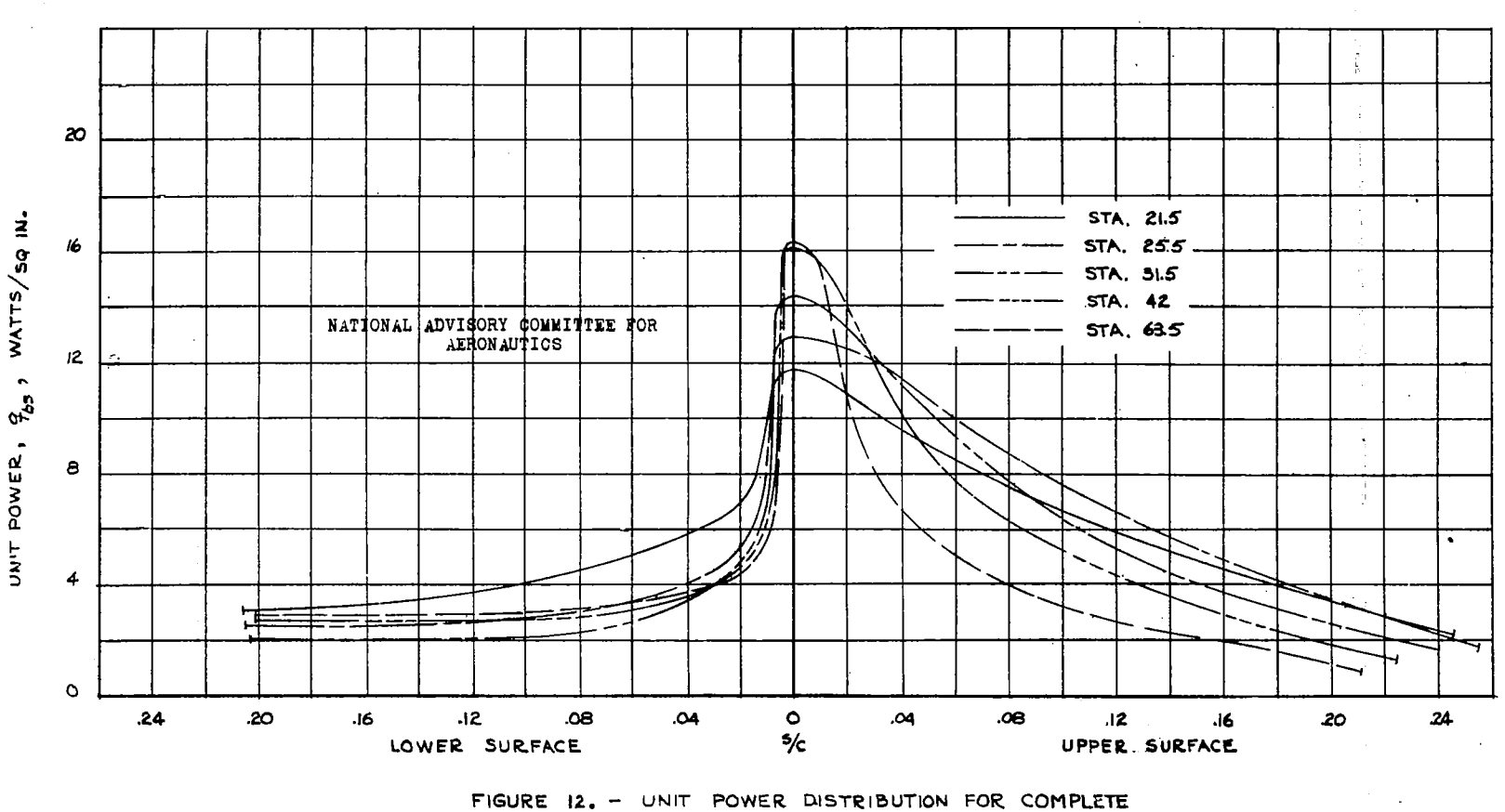

FIGURE 12. - UNIT POWER DISTRIBUTION FOR COMPLETE ICE PREVENTION.

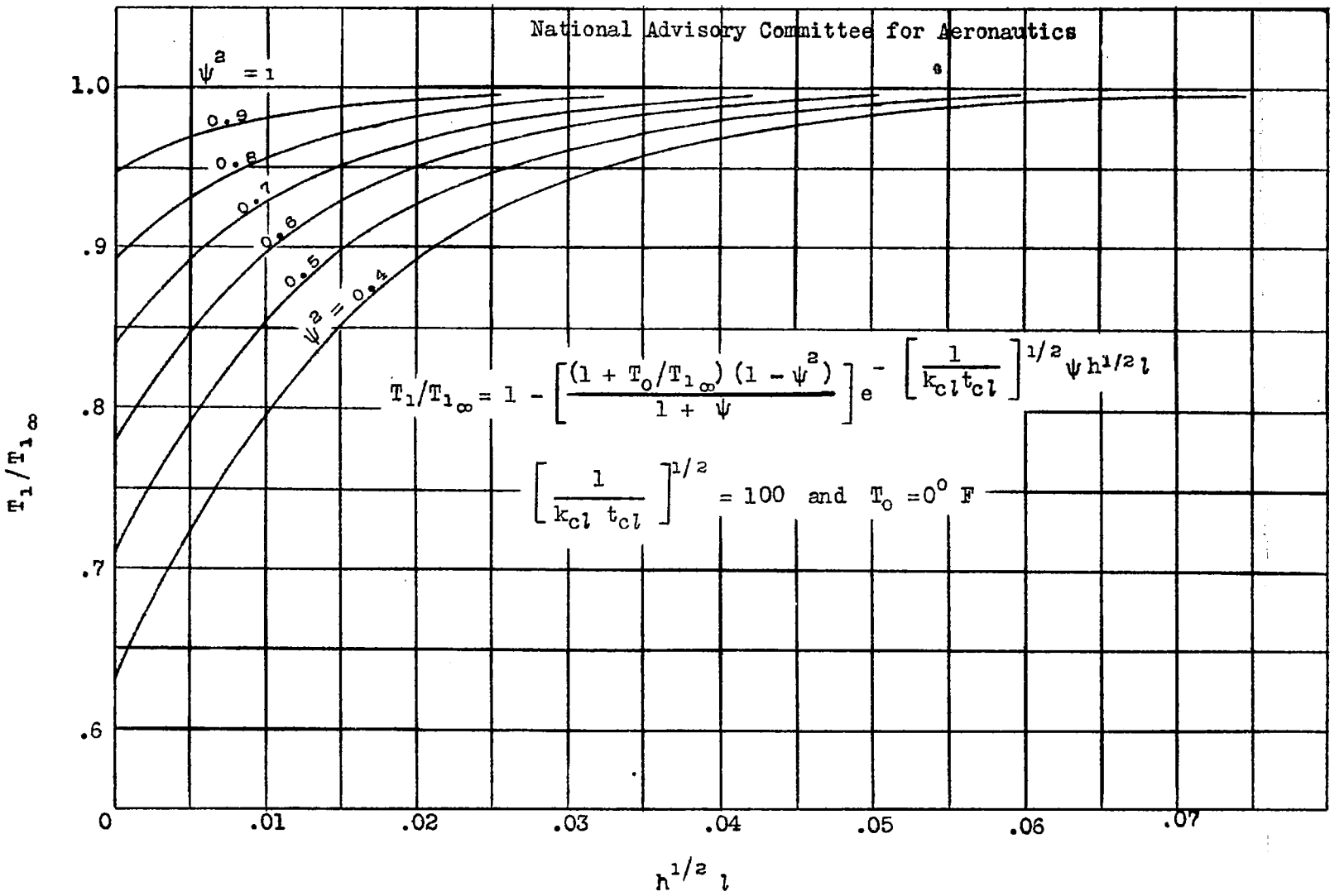

Figure 13.- Temperature gradient at the edge of an ice particle.

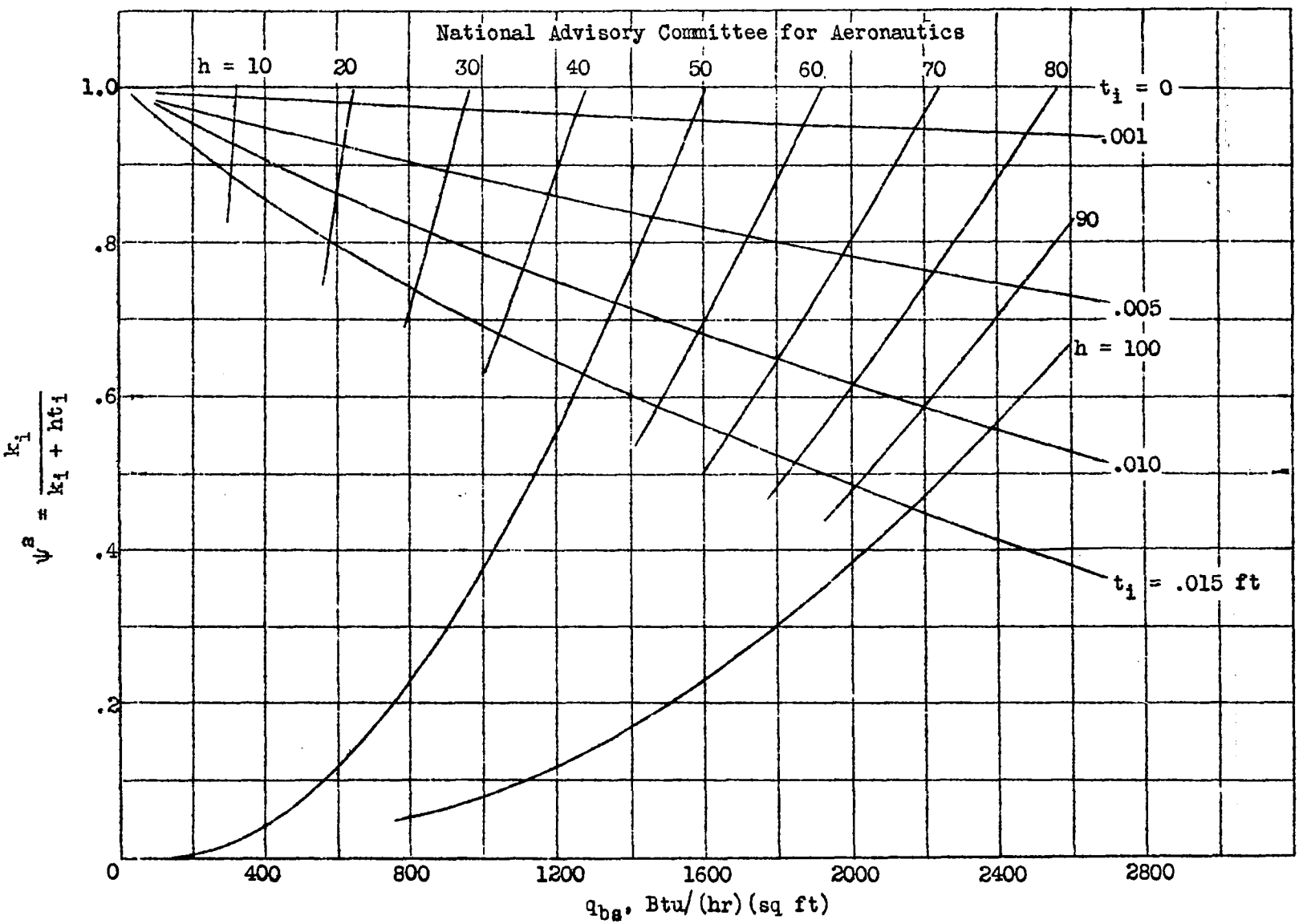

Figure 14.- Heat required to remove an ice particle .3 inch in diameter (T_o = 0° F), neglecting aerodynamic heating.

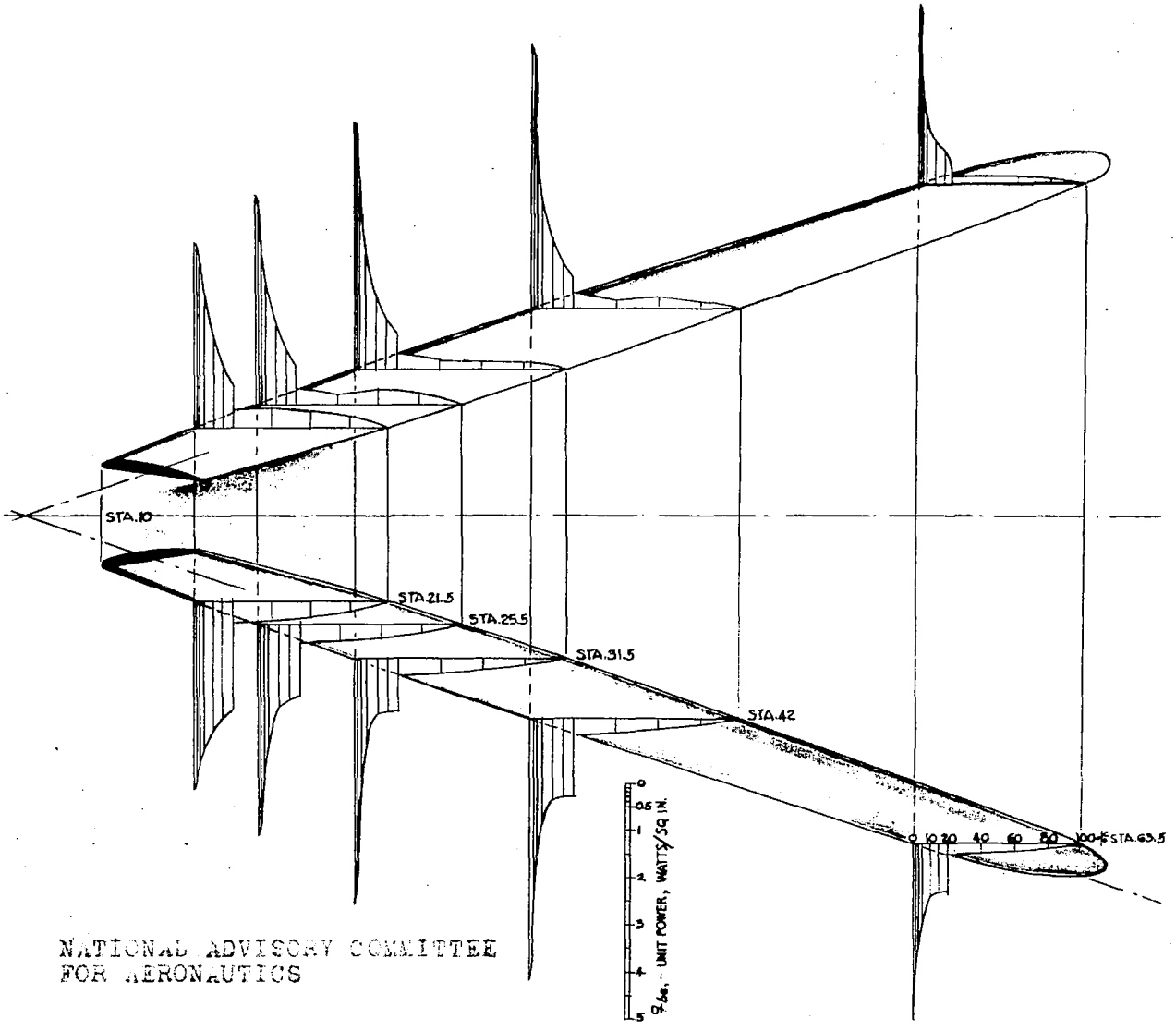

FIGURE 15.- UNIT POWER DISTRIBUTION ON THE HAMILTON STANDARD PROPELLER BLADE Nº 6477A-0 FOR ICE-PROTECTION AT THE DESIGN CONDITIONS.

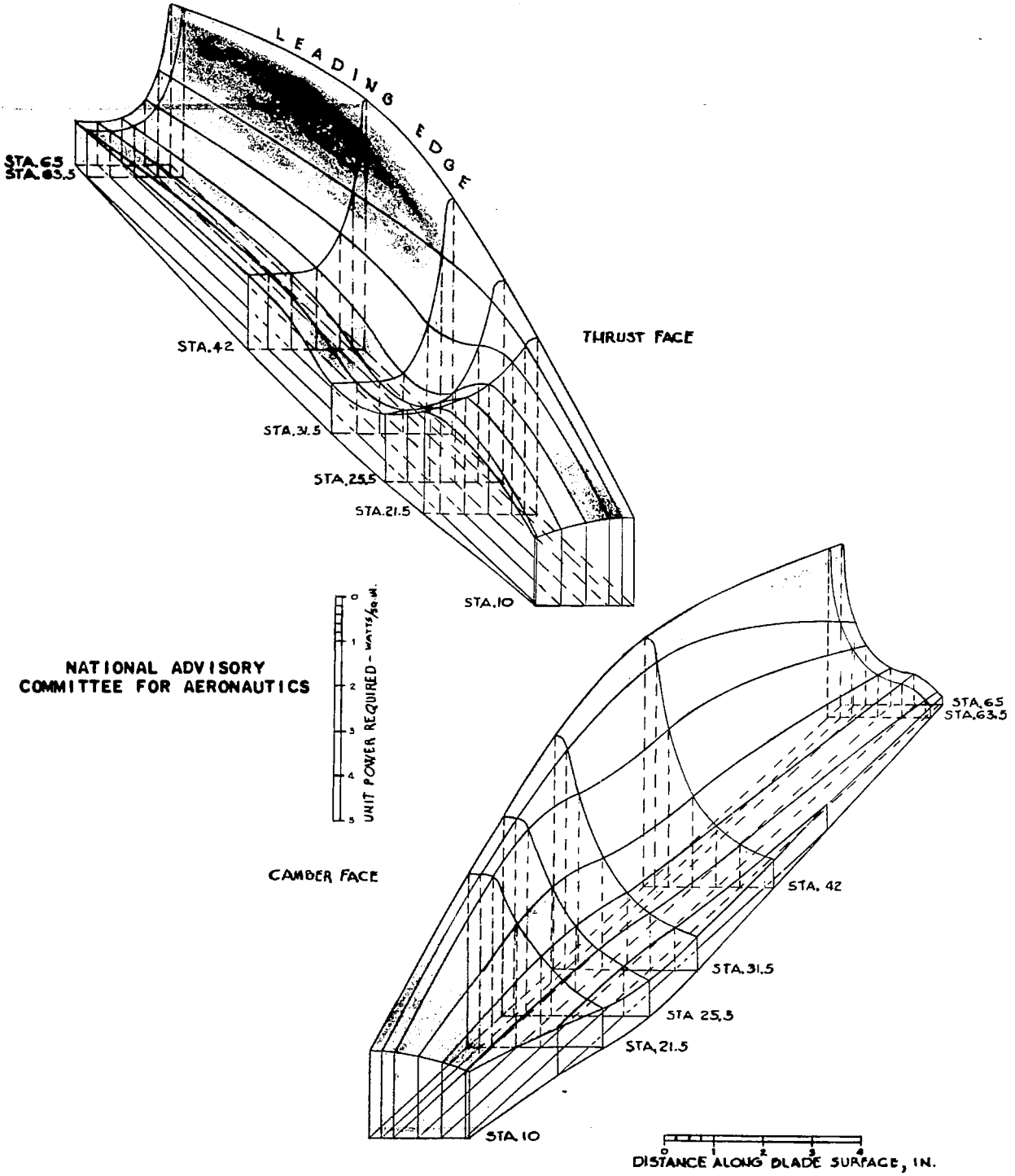

FIGURE 16. - UNIT POWER DISTRIBUTION ON THE BLADE SHOE SURFACE FOR ICE-PROTECTION FOR THE HAMILTON STANDARD PROPELLER BLADE NO 6477A-0 AT THE DESIGN CONDITIONS.

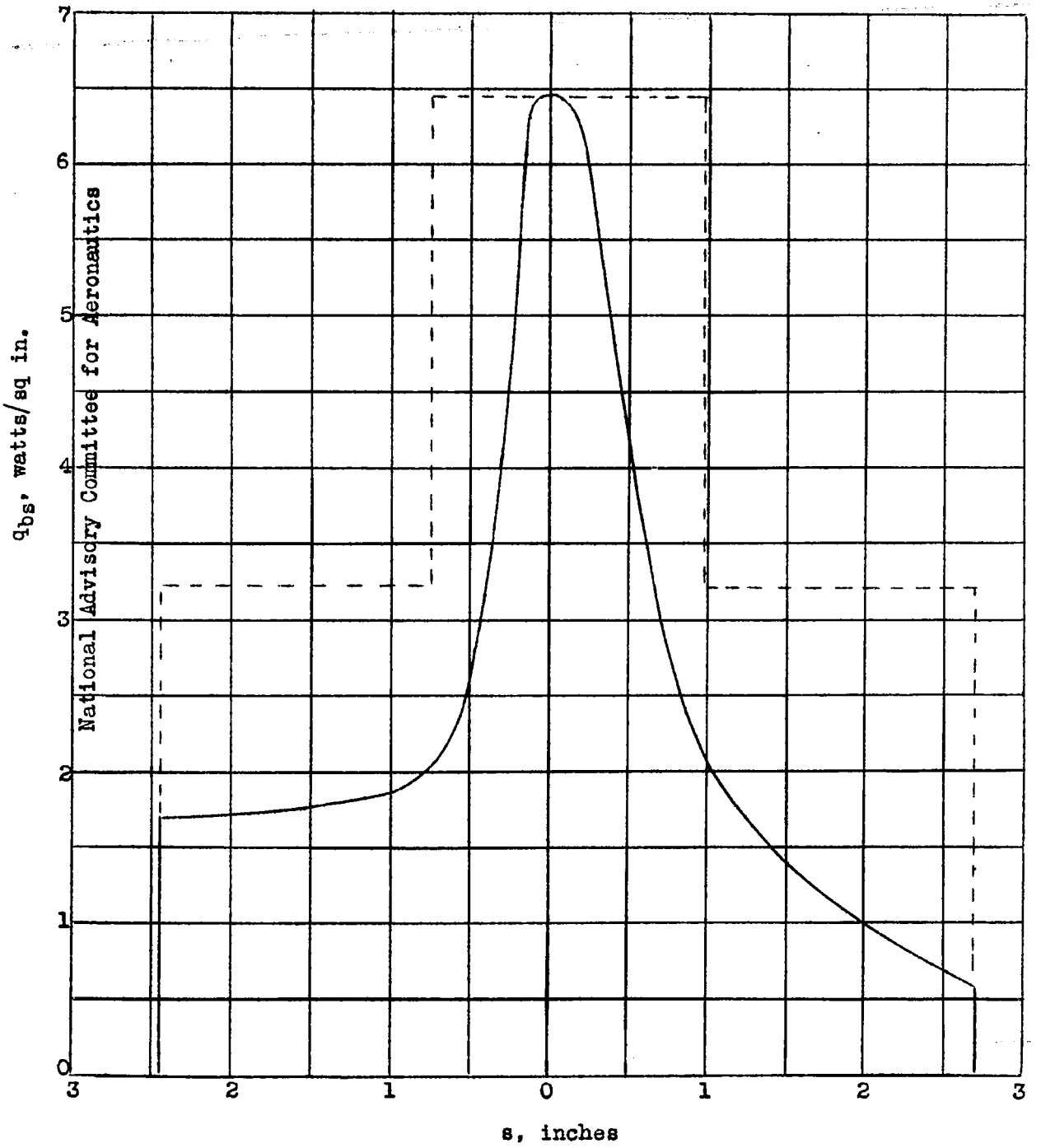

Figure 17.- Comparison of the stepped and optimum unit power distributions at station 42.